รายงานวิจัยฉบับสมบูรณ์

Final Report

โครงการ
การโก่งเดาะของเสาที่ทำจากวัสดุที่รับแรงในแต่ละทิศทางได้ไม่เท่ากัน – ด้วยหลักการไฮเปอร์อิลาสติก
Buckling of Anisotropic Columns – A Hyperelastic Formulation

โดย

ผศ.ดร.กริสน์ ชัยมูล

Asst. Prof. Krit Chaimoon, Ph.D.

มกราคม 2557

January 2014

สัญญาเลขที่ MRG5280018

รายงานวิจัยฉบับสมบูรณ์

โครงการ
การโก่งเดาะของเสาที่ทำจากวัสดุที่รับแรงในแต่ละทิศทางได้ไม่เท่ากัน – ด้วยหลักการไฮเปอร์อิลาสติก

ผู้วิจัย	สังกัด
1. ผศ.ดร.กริสน์ ชัยมูล (หัวหน้าโครงการ)	คณะวิศวกรรมศาสตร์ มหาวิทยาลัยมหาสารคาม
2. Asso.Prof. Mario M. Attard, Ph.D. (ที่ปรึกษา)	University of New South Wales, Australia
3. ศ.ดร.ปริญญา จินดาประเสริฐ (ที่ปรึกษา)	คณะวิศวกรรมศาสตร์ มหาวิทยาลัยขอนแก่น

สนับสนุนโดยสำนักงานคณะกรรมการการอุดมศึกษาและสำนักงานกองทุนสนับสนุนการวิจัย

บทคัดย่อ

รหัสโครงการ: MRG5280018

ชื่อโครงการ: การโก่งเดาะของเสาที่ทำจากวัสดุที่รับแรงในแต่ละทิศทางได้ไม่เท่ากัน – ด้วยหลักการไฮเปอร์อิลาสติก

ชื่อนักวิจัย และสถาบัน: ผศ.ดร.กริสน์ ชัยมูล คณะวิศวกรรมศาสตร์ มหาวิทยาลัยมหาสารคาม

อีเมล์: k.chaimoon@msu.ac.th

ระยะเวลาโครงการ: 15/03/2552 – 15/01/2557

บทคัดย่อ:

วัตถุประสงค์ของการศึกษานี้ คือ เพื่อที่จะหาฟังก์ชั่นพลังงานความเครียด (strain energy function) สำหรับวัสดุแอนไอโซโทรปิก (anisotropic) ซึ่งเป็นวัสดุที่รับแรงในแต่ละทิศทางได้ไม่เท่ากัน และมีการเสียรูปมาก และเพื่อที่จะหาสมการการโก่งเดาะของเสาแอนไอโซโทรปิก ซึ่งรวมการเสียรูปเนื่องจากแรงเฉือนด้วย สมการพลังงานความเครียดได้จากทฤษฎีไม่แปรผัน (invariant theory) โดยแสดงแอนไอโซโทรปีในรูปของฟังก์ชั่นไอโซโทรปิกเทนเซอร์ (isotropic tensor function) ผ่านทางเทนเซอร์ที่เรียกว่า structural tensor และสมการดังกล่าวได้พิจารณาเงื่อนไขของโพลีคอนเวกซิตี้ (polyconvexity) และโคเออซิวิตี้ (coercivity) เพื่อให้แน่ใจว่ามีคำตอบ ฟังก์ชั่นพลังงานความเครียดประกอบด้วยสองส่วนคือ ส่วนที่เป็นไอโซโทรปิกและส่วนที่เป็นแอนไอโซโทรปิก สมการการโก่งเดาะของเสาแอนไอโซโทรปิกถูกหาโดยใช้ฟังก์ชั่นพลังงานความเครียดที่ได้

คำหลัก : แอนไอโซโทรปี, ความเครียดจำกัด, พลังงานความเครียด, การโก่งเดาะของเสา

Abstract

Project Code : MRG5280018

Project Title : Buckling of anisotropic columns – A hyperelastic formulation

Investigator : Assistant Professor Krit Chaimoon, Ph.D.

E-mail Address : k.chaimoon@msu.ac.th

Project Period : 15/03/2009 – 15/01/2014

Abstract:

The aims of this study are to derive strain energy function for anisotropic hyperelastic materials under finite strain and to determine buckling equation which includes shear deformations for anisotropic columns. A generalized strain energy function is formulated within the framework of the invariant theory by representing the anisotropy using an isotropic tensor function through the so-called structural tensors and is based on polyconvexity and coercivity conditions so as to guarantee the existence of solutions. Furthermore, the strain energy density is decomposed into an isotropic and anisotropic component. The proposed strain energy density is then adopted to determine buckling equation which includes shear deformations for anisotropic columns.

Keywords : anisotropy, finite strain, hyperelasticity, strain energy, column buckling

Executive Summary

Being of a fundamental and innovative nature the proposed research will have importance for any finite strain elasticity analysis for both incompressible and compressible anisotropic materials. The application of anisotropic hyperelastic constitutive modeling to several buckling and postbuckling problems which include shear deformations will result a better prediction of the buckling capacity of anisotropic columns and will benefit the industrial use of such materials.

In this study, strain energy function for anisotropic hyperelastic materials under finite strain is formulated and buckling equation which includes shear deformations for anisotropic columns is determined.

Contents

Chapter 1

Introduction

1.1 Problems Statement

Many materials which are widely used in industries such as building, aircraft, aerospace, marine and biological technology can undergo large nonlinear elastic deformations and have inherent anisotropic characteristics. Examples of these materials are rubbers, rubber-like materials, foams, elastomers, fibre composites, sandwich panels and biological tissues. To be able to utilize these materials efficiently and economically, better analytical methods and designs are needed. Buckling analysis is fundamental to analysis, design and safety assessment of many structures. The inclusion of shear deformation in buckling analysis has proven problematic. Many traditional bucklikng formulations are incorrect when used to account for shear deformations. Shear deformations in buckling analyses are important considerations for the design of helical springs, sandwich plates with soft shear cores, built-up and laced columns and elastomeric bearings. Shear deformations during buckling are also important in the analysis of the compressive strength of the fiber composites. The constitutive material laws and a consistent large deflection formulation are crucial for a proper buckling analysis and challenge to the analyst, especially for anisotropic materials. Hyperelastic constitutive modeling has appeared as an effective tool in continuum mechanics for characterizing large deformation (finite strain) materials. The major aim of this research is to determine new fundamental expressions for the buckling formulas which include shear deformations for anisotropic columns based on a hyperelastic formulation.

1.2 Objectives

(1) To derive strain energy functions for anisotropic hyperelastic materials under finite strain.

(2) To establish anisotropic constitutive relationships using the developed strain energy functions.

(3) To determine buckling equations which include shear deformations for anisotropic columns.

1.3 Scope of Works

This study is focused only on developing a computational basis using a hyperelastic formulation, no experiment carried out, for assessing buckling capacity of large nonlinear elastic columns made of anisotropic materials under static loading.

1.4 Expected Outcomes

Being of a fundamental and innovative nature the proposed research will have importance for any finite strain elasticity analysis for both incompressible and compressible anisotropic materials. The application of anisotropic hyperelastic constitutive modeling to several buckling and postbuckling problems which include shear deformations will result a better prediction of the buckling capacity of anisotropic columns and will benefit the industrial use of such materials.

Chapter 2

Literature Review

2.1 Continuum Mechanics

2.1.1 Kinematics

Particles within a continuum of material at rest in an undeformed state can be thought of as forming natural lines or chains of particles called material lines [1]. If the material is deformed these chains of particles move in such a way that particles remain on the same material line, that is material lines always remain intact. Coordinates of a particle P within this continuum with respect to a fixed three-dimensional Cartesian coordinate system are normally assumed to be a function of general coordinates s^i, $i = 1,2,3$ as

$$x^i\left(s^1, s^2, s^3\right) \quad , \quad i = 1, 2, 3. \tag{1}$$

The s^i can be viewed as curvilinear or intrinsic coordinates along the material lines. The convention due to Einstein is adopted where a repeated index such as $p_i v^i$ is used to imply summation. A bracketed index indicates suppression of the summation convention, e.g. $x_{(ii)}$. The position vector $\mathbf{s}$ of the particle P in the undeformed state is given by

$$\mathbf{s} = \mathbf{i}_i x^i\left(s^1, s^2, s^3\right), \tag{2}$$

where $\mathbf{i}_i$ are unit Cartesian vectors (refer to Fig. 1). The bold style such as $\mathbf{s}$ is used to distinguish a vector while vector components will be written in italics, e.g. x^i.

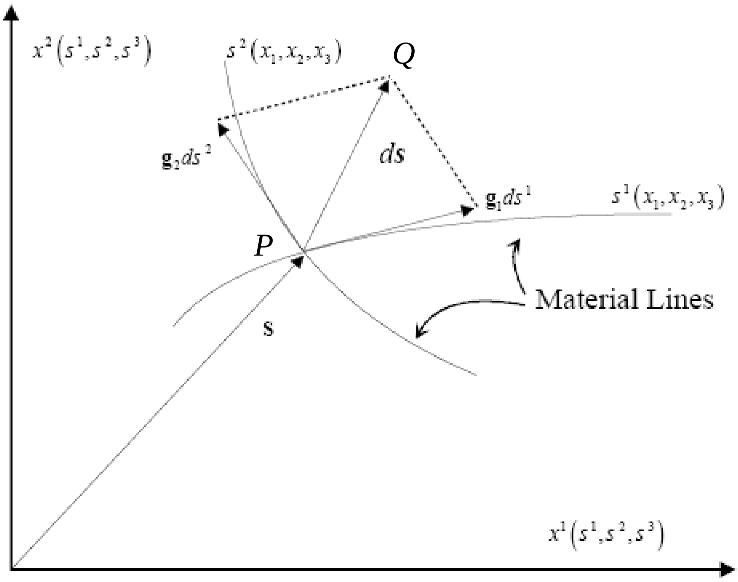

Fig. 1 Undeformed position

To examine deformations of the continuum a differential line element vector $d\mathbf{s}$ at the particle P in the undeformed state can be defined as

$$d\mathbf{s} = \frac{\partial \mathbf{s}}{\partial s^i} ds^i = \frac{\partial x^j}{\partial s^i} \mathbf{i}_j ds^i = x^j,_i \mathbf{i}_j ds^i = \mathbf{g}_i ds^i, \tag{3}$$

where $\mathbf{g}_i$ are the covariant tangent base vectors and ds^i are the contravariant vector components. The comma notation indicates differentiation with respect to s^i. The tangent base vectors are so-called because they are tangential to the natural material lines. These base vectors are not necessarily unit vectors and may not be dimensionless. The contravariant base vectors $\mathbf{g}^j$ are normal to the material lines and are sometimes referred to as reciprocal base vectors. The scalar product of covariant and contravariant base vectors is the kronecker delta δ_i^j,

$$\mathbf{g}_i \cdot \mathbf{g}^j = \mathbf{g}^j \cdot \mathbf{g}_i = \delta_i^j. \tag{4}$$

2.1.2 The Metric Tensor

The scalar length of the differential line element squared is called the metric and is calculated from

$$d\mathbf{s} \cdot d\mathbf{s} = \mathbf{g}_i \cdot \mathbf{g}_j ds^i ds^j = g_{ij} ds^i ds^j = ds_j ds^j, \tag{5}$$

where g_{ij} is the covariant metric tensor in the undeformed coordinate system and is symmetric.

2.1.3 Stretch

The position vector $\hat{\mathbf{s}}$ of a new position $\hat{P}$ (refer to Fig. 2) after moving of the particle P can be given by

$$\hat{\mathbf{s}} = \mathbf{s} + \mathbf{u}, \tag{6}$$

in which $\mathbf{u}$ are displacements assumed to be smooth and differentiable. The new position is also assumed to be a function of the coordinates s^i and therefore said to be convected coordinates (see e.g. [2]) as all positions are referred to the same coordinate.

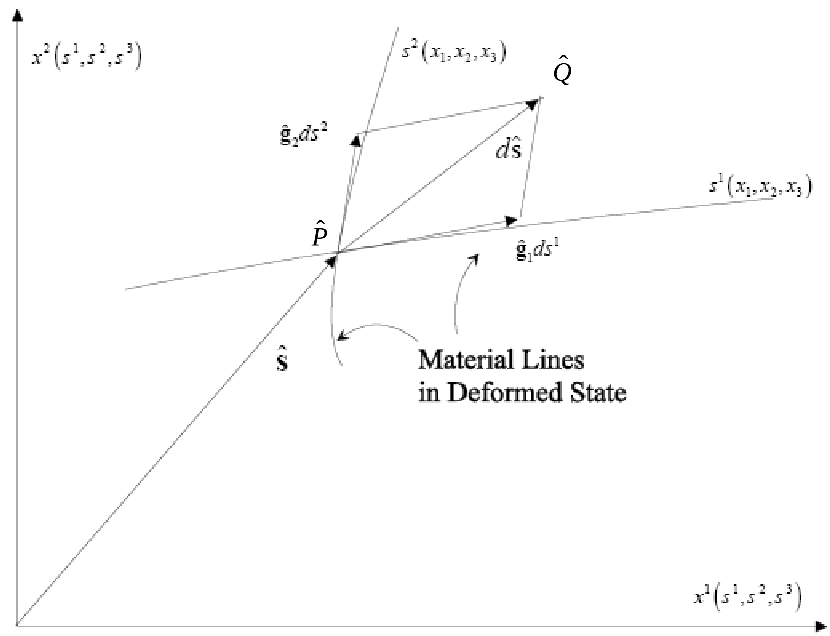

Fig. 2 Deformed position

A differential line element vector $d\hat{\mathbf{s}}$ at the particle $\hat{P}$ in the deformed state can be given by

$$d\hat{\mathbf{s}} = \frac{\partial \hat{\mathbf{s}}}{\partial s^i} ds^i = \hat{\mathbf{g}}_i ds^i = \mathbf{F} d\mathbf{s} = F_i^{\ j} \mathbf{g}_j ds^i, \tag{7}$$
$$\mathbf{F} = \hat{\mathbf{g}}_i \otimes \mathbf{g}^i = \left(\delta_i^j + u^j\big|_i\right) \mathbf{g}_j \otimes \mathbf{g}^i = \mathbf{I} + \nabla \otimes \mathbf{u},$$

where $\hat{\mathbf{g}}_i = \left(\delta_i^j + u^j\big|_i\right)\mathbf{g}_j$ are the covariant tangent base vectors in the deformed state, δ_i^j is the kronecker delta, $\mathbf{I} = \mathbf{g}_i \otimes \mathbf{g}^i$ is the identity tensor, $\nabla \otimes \mathbf{u} = u^j\big|_i \mathbf{g}_j \otimes \mathbf{g}^i$ is the grad of the displacement vector, $\mathbf{g}_i$ and $\mathbf{g}^i$ are the contravariant and covariant initial base vectors, respectively, in the undeformed state, $u^j\big|_i$ represent the covariant derivatives of the u^j vector component with respect to the coordinate corresponding to the index i and $\mathbf{F}$ is the deformation gradient tensor.

For an initial Cartesian coordinate system x, y and z, covariant and contravariant components with respect to the initial base vectors are not different and therefore the components of the deformation tensor can be written in matrix form as

$$\mathbf{F} = \begin{bmatrix} 1+u_{1,1} & u_{1,2} & u_{1,3} \\ u_{2,1} & 1+u_{2,2} & u_{2,3} \\ u_{3,1} & u_{3,2} & 1+u_{3,3} \end{bmatrix}, \tag{8}$$

where u_1, u_2 and u_3 are displacement components in the x, y and z directions, respectively, and $u_{1,x}$ symbolizes differentialtion with respect to x.

The stretch is the ratio of the change in lengths of the sides of the parallelepiped to their initial length as P moves to $\hat{P}$ and can be expressed as

$$\left|\hat{\mathbf{g}}_1 ds^1\right| = \sqrt{\hat{g}_{11}} = \lambda_1 \left|\mathbf{g}_1 ds^1\right| = \lambda_1\sqrt{g_{11}}, \tag{9}$$

$$\lambda_i = \sqrt{\frac{\hat{g}_{(ii)}}{g_{(ii)}}}, \tag{10}$$

where $g_{(ii)}$ and $\hat{g}_{(ii)}$ are the ith covariant material arcs in undeformed and deformed state, respectively. The λ_i is not a tensor and must be positive for all deformations $(\lambda_i > 0)$.

2.1.4 The right Cauchy-Green deformation tensor

The square of the length of the differential line element in the deformed configuration at the particle $\hat{P}$ can be expressed in terms of the square of the length of the differential line element in the undeformed state and is given by

$$\begin{aligned} d\hat{\mathbf{s}} \cdot d\hat{\mathbf{s}} &= d\mathbf{s} \cdot \mathbf{F}^{\mathrm{T}}\mathbf{F} \cdot d\mathbf{s} = d\mathbf{s} \cdot \mathbf{C} \cdot d\mathbf{s} \\ &= \hat{\mathbf{g}}_i ds^i \cdot \hat{\mathbf{g}}_j ds^j = \hat{g}_{ij} ds^i ds^j, \end{aligned} \tag{11}$$

where $\mathbf{C}=\mathbf{F}^{\mathrm{T}}\mathbf{F}$ is the right Cauchy-Green deformation tensor and is symmetric if invertible positive definite. A rigid motion at a point would correspond to $|d\hat{\mathbf{s}}|=|d\mathbf{s}|\ \therefore\ \mathbf{C}=\mathbf{I}$. For the three dimensional case, the components of $\mathbf{C}$ can be written in terms of the stretches ($\lambda_1,\lambda_2\ \&\ \lambda_3$) and angles between the tangent base vectors in the deformed state ($\varphi_{12},\varphi_{13}\ \&\ \varphi_{23}$) [3], that is

$$\mathbf{C}=\begin{bmatrix} (\lambda_1)^2 & \lambda_1\lambda_2\cos\varphi_{12} & \lambda_1\lambda_3\cos\varphi_{13} \\ \lambda_1\lambda_2\cos\varphi_{12} & (\lambda_2)^2 & \lambda_2\lambda_3\cos\varphi_{23} \\ \lambda_1\lambda_3\cos\varphi_{13} & \lambda_2\lambda_3\cos\varphi_{23} & (\lambda_3)^2 \end{bmatrix}, \tag{12}$$

2.1.5 The Green Strain Tensor

The change in length of the square of the differential line element can be used to characterize any distortion or deformation and is used to define a Green or Lagrangian strain tensor Σ by

$$\begin{aligned} |d\hat{\mathbf{s}}|^2-|d\mathbf{s}|^2 &= d\hat{\mathbf{s}}\cdot d\hat{\mathbf{s}}-d\mathbf{s}\cdot d\mathbf{s} \\ &= d\mathbf{s}\cdot(\mathbf{C}-\mathbf{I})\cdot d\mathbf{s}=2d\mathbf{s}\cdot\Sigma\cdot d\mathbf{s}. \end{aligned} \tag{13}$$

The Green strain tensor is given by

$$\Sigma=\frac{1}{2}(\mathbf{C}-\mathbf{I}). \tag{14}$$

2.1.6 Stress Tensors

Within the continuum there are internal forces necessary to keep the body in equilibrium. An infinitesimal force vector $d\mathbf{p}$ at the point $\hat{P}$ can be written in the form

$$d\mathbf{p}=d\hat{p}^j\hat{\mathbf{g}}_j=dp^j\mathbf{g}_j=d\hat{\mathbf{T}}^i d\hat{A}_i=d\mathbf{T}^i dA_i=d\overline{\mathbf{T}}^i d\overline{A}_i, \tag{15}$$

where $d\hat{p}^j$ and dp^j are the contravariant force vector components with respect to base vectors in the deformed and undeformed configuration, respectively, $d\hat{\mathbf{T}}^i, d\overline{\mathbf{T}}^i$ and $d\mathbf{T}^i$ are the stress vector components acting on the faces of the infinitesimal parallelepiped at the point $\hat{P}$, and $d\hat{A}_i, d\overline{A}_i$ and dA_i are the area vector components defined by

$$d\hat{\mathbf{A}} = d\hat{A}_i \hat{\mathbf{g}}^i = d\bar{A}_i \mathbf{g}^i, \quad d\mathbf{A} = dA_i \mathbf{g}^i,$$
$$d\hat{A}_i = J dA_i, \quad d\bar{A}_i = \bar{F}_i^{\ j} d\hat{A}_j, \quad \bar{F}_i^{\ j} = \left(F_i^{\ j}\right)^{-1}, \tag{16}$$

where $d\hat{\mathbf{A}}$ and $d\mathbf{A}$ are area vectors in the deformed and undeformed state, respectively, and $J = \det \mathbf{F}$ is volumetric invariant or Jacobian. Some of the common stress tensors are defined by

$$d\mathbf{p} = \tau^{ij} \hat{\mathbf{g}}_j d\hat{A}_i = \pi^{ij} \hat{\mathbf{g}}_j dA_i = t^{ij} \mathbf{g}_j dA_i = \sigma^{ij} \mathbf{g}_j d\bar{A}_i, \tag{17}$$

where τ^{ij} is the component of the Eulerian stress tensor $\boldsymbol{\tau}$, π^{ij} is the component of the second Piola-Kirchhoff stress tensor $\boldsymbol{\pi}$, t^{ij} is the component of the first Piola-Kirchhoff stress tensor $\mathbf{t}$, and σ^{ij} is the component of the Cauchy stress tensor $\boldsymbol{\sigma}$. The Eulerian stress tensor, the second Piola-Kirchhoff stress tensor and the Cauchy stress tensor are all symmetric. The stress tensors are related by

$$\tau^{ij} J = \pi^{ij}, \quad \sigma^{ij} = F_m^{\ i} F_n^{\ j} \tau^{mn}, \quad t^{ij} = \pi^{ir} F_r^{\ j}$$
$$\text{or} \quad J\boldsymbol{\tau} = \boldsymbol{\pi}, \quad \boldsymbol{\sigma} = \mathbf{F}\boldsymbol{\tau}\mathbf{F}^T, \quad \mathbf{t} = \boldsymbol{\pi}\mathbf{F}^T. \tag{18}$$

The stress tensors do not necessarily have units of force per unit area.

2.2 Hyperelastic Strain Energy Function

Hyperelastic material is an elastic material that its elastic behavior can be described by a strain energy density $W = W(\mathbf{F})$ with respect to the initial volume.

In order to purpose a strain energy density in which anisotropy is taken into account, the following postulates, as to conditions to which the anisotropic strain energy density must hold [4], must be taken into consideration for formulating the strain energy density:

(1) The strain energy density must meet the objectivity condition (the principle of material frame indifference).

(2) The strain energy density must take into account the principle of material symmetry.

(3) In order to guarantee the existence of solutions, the strain energy density must be sequentially weakly lower semicontinuous (s.w.l.s.) and must meet a coercivity condition.

(4) The strain energy density must meet the ellipticity condition which is a possible criterion for material stability.

(5) The strain energy density must satisfy the stress free reference configuration condition.

2.2.1 Objectivity

This condition implies that the strain energy density has to be independent of superposed rigid body motions and can automatically be met by representing the strain energy function in terms of the right Cauchy-Green deformation tensor $\mathbf{C}$ so that (see e.g. [5])

$$W = W\left(\mathbf{F}\right) = W(\mathbf{C}). \tag{19}$$

Accordingly, a constitutive law for a hyperelastic material can be obtained from

$$\boldsymbol{\pi} = 2\frac{\partial W}{\partial \mathbf{C}}. \tag{20}$$

2.2.2 Material symmetry

This condition requires that the strain energy density be invariant under transformations with elements of the material symmetry group which describes the anisotropy class of the material. Following the Rychlewski's theorem [6], the strain energy density has to be represented as an isotropic tensor function of arguments containing the so-called structural tensors which are symmetric and positive definite. This allows an invariant formulation. In this context see also [7, 8]. In order to meet both the objectivity condition and the principle of material symmetry, the strain energy density is thus written in terms of the right Cauchy-Green deformation tensor and the structural tensors, and also has to satisfy

$$W = W(\mathbf{C}, \mathbf{G}_i) = W(\mathbf{Q}\mathbf{C}\mathbf{Q}^T, \mathbf{Q}\mathbf{G}_i\mathbf{Q}^T), \tag{21}$$

which is an isotropic tensor function in the arguments $(\mathbf{C}, \mathbf{G}_i)$ where $\mathbf{G}_i, i = 0,1,...,n$ are the structural tensors and $\mathbf{Q}$ is an element of the material symmetry group and is a proper orthogonal tensor. With this the invariance of $W = W(\mathbf{C}, \mathbf{G}_i)$ with respect to the symmetry transformations is ensured. Thus superimposed rigid body motions do not either affect the behavior of the anisotropic material.

2.2.3 Structual tensors

A definition for the structural tensors $\mathbf{G}_i$ is required for this method. Following Zheng and Boehler [9], anisotropy can be characterized by certain directions, lines or planes associated with some unit vectors defined in the undeformed state. This leads to a definition for the structural tensors $\mathbf{G}_i$ of the form

$$\mathbf{G}_i = \mathbf{m}_i \otimes \mathbf{m}_i, \tag{22}$$

where each $\mathbf{m}_i,\ i = 1, 2, ..., n$ is a unit vector. The structural tensors, which are symmetric and positive definite, have the property

$$\operatorname{tr}\left[\mathbf{G}_i\right] = 1, \tag{23}$$

where $\operatorname{tr}(.)$ denotes the trace function.

2.2.4 Invariants

For the invariant formulation of constitutive equations the invariants of the right Cauchy-Green deformation tensor and the structural tensors are needed. Based on the Hilbert's theorem, a finite set of isotropic invariants of these tensors can be obtained [10]. In general the invariants contain the traces of products of powers of the argument tensors, the so-called principal invariants and the so-called mixed invariants. The invariants of a single tensor for two symmetric second order tensors $\mathbf{C}$ and $\mathbf{G}_i$ may consist of

$$J_1 = \operatorname{tr}\left[\mathbf{C}\right], \quad J_2 = \operatorname{tr}\left[\mathbf{C}^2\right], \quad J_3 = \operatorname{tr}\left[\mathbf{C}^3\right], \tag{24}$$

$$J_{4i} = \operatorname{tr}\left[\mathbf{C}\mathbf{G}_i\right], \quad J_{5i} = \operatorname{tr}\left[\mathbf{C}^2\mathbf{G}_i\right], \quad J_{6i} = \operatorname{tr}\left[\mathbf{C}\mathbf{G}_i^2\right], \quad J_{7i} = \operatorname{tr}\left[\mathbf{C}^2\mathbf{G}_i^2\right], \tag{25}$$

$$J_{8i} = \operatorname{tr}\left[\mathbf{G}_i\right], \quad J_{9i} = \operatorname{tr}\left[\mathbf{G}_i^2\right], \quad J_{10i} = \operatorname{tr}\left[\mathbf{G}_i^3\right], \tag{26}$$

where the invariants in Eq. (24) are the so-called basic invariants defined by the traces of powers of $\mathbf{C}$, the invariants in Eq. (25) are the mixed invariants for $\mathbf{C}$ and $\mathbf{G}_i$, and the invariants in Eq. (26) are the traces of powers of $\mathbf{G}_i$. The basic invariants can also be related to the principal invariants of $\mathbf{C}$ by

$$J_1 = I_1, \quad J_2 = I_1^2 - 2I_2, \quad J_3 = I_1^3 - 3I_1I_2 + 3I_3, \tag{27}$$

where I_1, I_2 and I_3 are the principal invariants of $\mathbf{C}$ and have the explicit expressions as

$$I_1 = \mathrm{tr}\left[\mathbf{C}\right] = \mathbf{I}\cdot\mathbf{C} = \left(\lambda_{p1}\right)^2 + \left(\lambda_{p2}\right)^2 + \left(\lambda_{p3}\right)^2, \tag{28}$$

$$\begin{aligned} I_2 &= \mathrm{tr}\left[\mathrm{Cof}\left[\mathbf{C}\right]\right] = \mathbf{I}\cdot\mathrm{Cof}\left[\mathbf{C}\right] = \frac{1}{2}\left\{\left(\mathrm{tr}\left[\mathbf{C}\right]\right)^2 - \mathrm{tr}\left[\mathbf{C}^2\right]\right\} \\ &= \left(\lambda_{p1}\lambda_{p2}\right)^2 + \left(\lambda_{p2}\lambda_{p3}\right)^2 + \left(\lambda_{p3}\lambda_{p1}\right)^2, \end{aligned} \tag{29}$$

$$I_3 = \det\left[\mathbf{C}\right] = \frac{1}{6}\left\{\left(\mathrm{tr}\left[\mathbf{C}\right]\right)^3 - 3\mathrm{tr}\left[\mathbf{C}\right]\mathrm{tr}\left[\mathbf{C}^2\right] + 2\mathrm{tr}\left[\mathbf{C}^3\right]\right\} = \left(\lambda_{p1}\lambda_{p2}\lambda_{p3}\right)^2, \tag{30}$$

where λ_{pi} are the principal stretches, $\mathrm{Cof}\left[\mathbf{C}\right]$ is the cofactor of $\mathbf{C}$ and is defined by $\mathrm{Cof}\left[\mathbf{C}\right] = \det\left[\mathbf{C}\right]\mathbf{C}^{-1} = \mathrm{Adj}\left[\mathbf{C}\right]$ for all invertible and isotropic $\mathbf{C}$ and $\det\left[\mathbf{C}\right]$ denotes the determinant of $\mathbf{C}$.

2.2.5 Sequential weak lower semicontinuity and coercivity

In order to guarantee the existence of solutions, the strain energy density must be sequentially weakly lower semicontinuous (s.w.l.s.) and must meet a coercivity condition. A discussion on this issue was made in [4] and the polyconvexity condition in the sense of Ball [11] has also been proved to be able to serve for both s.w.l.s. and coercivity conditions.

A strain energy density is said to be polyconvex [11] if and only if there exists a convex function with the arguments of $\mathbf{F}$, $\mathrm{Cof}\left[\mathbf{F}\right]$ and $\det\left[\mathbf{F}\right]$ in such a way that the strain energy density $W = W(\mathbf{F})$ can satisfy

$$W = W(\mathbf{F}) = W\left(\mathbf{F}, \mathrm{Cof}\left[\mathbf{F}\right], \det\left[\mathbf{F}\right]\right) \tag{31}$$

where $\mathrm{Cof}\left[\mathbf{F}\right]$ denotes the cofactor of $\mathbf{F}$ and is defined by $\mathrm{Cof}\left[\mathbf{F}\right] = \det\left[\mathbf{F}\right]\mathbf{F}^{-T} = \left(\mathrm{Adj}\left[\mathbf{F}\right]\right)^T$ for all invertible $\mathbf{F}$ and $\det\left[\mathbf{F}\right]$ denotes the determinant of $\mathbf{F}$. The arguments $\mathbf{F}$, $\mathrm{Cof}\left[\mathbf{F}\right]$ and $\det\left[\mathbf{F}\right]$ are the linear mappings of the infinitesimal line, area and volume elements according to the well-known Nanson's formula, respectively.

2.2.6 Ellipticity

Ellipticity condition is a possible criterion for material stability. It has been proved that polyconvexity implies ellipticity [12, 13]. Thus, ellipticity is automatically guaranteed for the strain energy function which has already fulfilled the polyconvexity condition.

Chapter 3

Hyperelastic Formulation of Strain Energy Functions

In this chapter, a generalized hyperelastic model for anisotropic materials is formulated and proposed. The mentioned postulates in the Chapter 2, as to conditions to which the anisotropic strain energy density must hold, are taken into consideration for formulating the strain energy function.

3.1 Hyperelastic Strain Energy Function

As described in Chapter 2, the strain energy functions must meet the objectivity condition (the principle of material frame- indifference) and the principle of material symmetry. In ordet to meet both conditions, the proposed strain energy function is thus written in terms of the right Cauchy-Green deformation tensor, $\mathbf{C}$, and the structural tensors, $\mathbf{G}_i$ as $W = W(\mathbf{C}, \mathbf{G}_i) = W(\mathbf{Q}\mathbf{C}\mathbf{Q}^T, \mathbf{Q}\mathbf{G}_i\mathbf{Q}^T)$, see Eq. (21).

For the formulation of the strain energy function, only a set of invariants is determined. Due to the property of the structural tensors in Eq. (23), the terms J_{6i} and J_{7i} in Eq. (25) can be discarded since $J_{6i} \equiv J_{4i}$ and $J_{7i} \equiv J_{5i}$. Besides, the basic invariants of $\mathbf{G}_i$, Eq. (26), are constants and can be neglected [10]. As a result, the strain energy function can be expressed in terms of the invariants of the argument tensors $(\mathbf{C}, \mathbf{G}_i)$ as

$$W = W(I_1, I_2, I_3, J_{4i}, J_{5i}). \tag{32}$$

This expression preserves the invariant of the strain energy function under all transformations.

As the polyconvexity condition has been proved to be able to serve for both s.w.l.s. and coercivity conditions. Furthermore, ellipticity condition is also guaranteed. Hence, the proposed strain energy function is formulated on the basis of the polyconvexity.

3.1.1 Polyconvex Strain Energy Functions

According to Eq.(31), a subclass of the equation is the additive polyconvex functions [4] of the form

$$W\left(\mathbf{F}, \mathrm{Cof}\left[\mathbf{F}\right], \det\left[\mathbf{F}\right]\right) = W_1\left(\mathbf{F}\right) + W_2\left(\mathrm{Cof}\left[\mathbf{F}\right]\right) + W_2\left(\det\left[\mathbf{F}\right]\right) \tag{33}$$

where $W_i, i=1,2,3$ are convex functions of their argument, respectively.

The definition of the polyconvexity requires the convexity properties of the arguments of the strain energy density. Consequently, we consider the convexity properties of the invariants in Eq. (32). The convexity of each invariant can be proved by the positivity of the second derivative. Indeed it can be shown that the invariants I_1, I_2, I_3 and J_{4i} are convex with respect to $\mathbf{F}$, $\mathrm{Cof}\left[\mathbf{F}\right]$, $\det\left[\mathbf{F}\right]$ and $\mathbf{F}$, respectively, but the invariant J_{5i} are not convex with respect to $\mathbf{F}$ [4]. Therefore, the strain energy density written in terms of the invariant J_{5i} as single term, Eq. (32), does not fulfill the polyconvexity condition. In order to allow for quadratic expression of the invariant J_{5i} within the strain energy density, a polyconvex mixed invariant has to be used instead which can be derived by use of the Cayley-Hamilton theorem [4]. On the basis of the Cayley-Hamilton theorem, the characteristic equation of the second order tensors $\mathbf{C}$ is

$$\mathbf{C}^3 - \mathrm{tr}\left[\mathbf{C}\right]\mathbf{C}^2 + \mathrm{tr}\left[\mathrm{Adj}\mathbf{C}\right]\mathbf{C} - \det\left[\mathbf{C}\right]\mathbf{I} = \mathbf{0}. \tag{34}$$

Multiplication of the Eq. (34) with $\mathbf{C}^{-1}\mathbf{G}_i$ yields with $\mathrm{Cof}\left[\mathbf{C}\right] = \mathrm{Adj}\left[\mathbf{C}\right]$

$$\mathbf{C}^2\mathbf{G}_i - I_1\mathbf{C}\mathbf{G}_i + I_2\mathbf{G}_i - \mathrm{Cof}\left[\mathbf{C}\right]\mathbf{G}_i = \mathbf{0}. \tag{35}$$

Taking the trace of the Eq. (35) leads to the expression

$$K_{5i} = \mathrm{tr}\left[\mathrm{Cof}\left[\mathbf{C}\right]\mathbf{G}_i\right] = J_{5i} - I_1 J_{4i} + I_2 \mathrm{tr}\left[\mathbf{G}_i\right], \tag{36}$$

where K_{5i} is a mixed invariant representing a quadratic expression and is particularly polyconvex with respect to $\mathrm{Cof}\left[\mathbf{F}\right]$. In order to automatically satisfy the polyconvexity condition, the expression for the strain energy density in Eq. (32) is, thus, replaced by

$$W = W(I_1, I_2, I_3, J_{4i}, K_{5i}). \tag{37}$$

In the next step, we utilize the additive representation of the polyconvexity, Eq. (33), to additively decompose the strain energy function, Eq. (37), into the isotropic W_{iso} and anisotropic W_{aniso} parts. In addition, the two parts are associated with scalar weight factors w_i representing a dispersion of components as experimentally observed, see e.g. [14], i.e.

$$W = w_0 \cdot W_{\text{iso}}\left(I_1, I_2, I_3\right) + \sum_{r=1}^{m}\sum_{i=1}^{n} w_i^r \cdot W_{\text{aniso}}^r\left(I_3, J_{4i}, K_{5i}\right), \qquad \sum_{r=1}^{m}\sum_{i=1}^{n} w_i^r = 1 - w_0. \tag{38}$$

Note that taking of linear combinations of the polyconvex invariants does not change the polyconvexity properties [13]. This decomposition of the strain energy function allows a variety of combinations of the two parts. The anisotropic part is given in terms of a series with an arbitrary numbers of terms r.

3.1.2 Natural State Conditions

In this section, the isotropic and anisotropic stain energy functions which fulfill the polyconvexity condition are defined and analyzed with respect to the natural state conditions, i.e. the stress and energy have to be zero in the undeformed configuration. Some specific functions are also presented.

3.1.2.1 Isotropic Strain Energy Function

For the isotropic part W_{iso} of Eq. (38), a generic form is considered and assumed to be decomposed into two components as

$$W_{\text{iso}}\left(I_1, I_2, I_3\right) = W_{\text{iso}}^{\text{inc}}\left(I_1, I_2, I_3\right) + W_{\text{iso}}^{\text{com}}\left(I_3\right), \tag{39}$$

where $W_{\text{iso}}^{\text{inc}}$ is an incompressible component associated with constrained volume change or volume constant distortion and $W_{\text{iso}}^{\text{com}}$ is a compressible component associated with specific volume change. The isotropic part of the second Piola-Kirchhoff stress tensor are then given by

$$\boldsymbol{\pi}_{\text{iso}} = 2\frac{\partial W_{\text{iso}}}{\partial \mathbf{C}} = 2\left[\left(\frac{\partial W_{\text{iso}}^{\text{inc}}}{\partial I_1} + \frac{\partial W_{\text{iso}}^{\text{inc}}}{\partial I_2} I_1\right)\mathbf{I} - \frac{\partial W_{\text{iso}}^{\text{inc}}}{\partial I_2}\mathbf{C} + \frac{\partial W_{\text{iso}}^{\text{inc}}}{\partial I_3} I_3\mathbf{C}^{-1} + \frac{\partial W_{\text{iso}}^{\text{com}}}{\partial I_3} I_3\mathbf{C}^{-1}\right], \tag{40}$$

with $\partial I_1/\partial \mathbf{C} = \mathbf{I}$, $\partial I_2/\partial \mathbf{C} = I_1\mathbf{I} - \mathbf{C}$ and $\partial I_3/\partial \mathbf{C} = I_3\mathbf{C}^{-1}$. In order to consider the stress condition for the natural state, $\mathbf{C} = \mathbf{I}$ is set and $\boldsymbol{\pi}_{\text{iso}}\big|_{\mathbf{C}=\mathbf{I}} = \mathbf{0}$ is required, i.e.,

$$\left(\frac{\partial W_{\text{iso}}^{\text{inc}}}{\partial I_1}+2\frac{\partial W_{\text{iso}}^{\text{inc}}}{\partial I_2}+\frac{\partial W_{\text{iso}}^{\text{inc}}}{\partial I_3}+\frac{\partial W_{\text{iso}}^{\text{com}}}{\partial I_3}\right)\mathbf{I}=\mathbf{0}, \tag{41}$$

with $I_1=3,\ I_2=3,\ \text{and}\ I_3=1$ at $\mathbf{C}=\mathbf{I}$. Thus, the stress-free conditions are

$$\frac{\partial W_{\text{iso}}^{\text{inc}}}{\partial I_1}+2\frac{\partial W_{\text{iso}}^{\text{inc}}}{\partial I_2}+\frac{\partial W_{\text{iso}}^{\text{inc}}}{\partial I_3}=-\frac{\partial W_{\text{iso}}^{\text{com}}}{\partial I_3}. \tag{42}$$

For the energy condition at undeformed configuration, $\mathbf{C}=\mathbf{I}$ is set and $W_{\text{iso}}\big|_{\mathbf{C}=\mathbf{I}}=\mathbf{0}$ is required, i.e.,

$$W_{\text{iso}}^{\text{inc}}\left(3,3,1\right)+W_{\text{iso}}^{\text{com}}(1)=0. \tag{43}$$

Thus, the energy-free conditions are

$$W_{\text{iso}}^{\text{inc}}\left(3,3,1\right)=-W_{\text{iso}}^{\text{com}}(1)=0. \tag{44}$$

For example, specific functions for the isotropic part W_{iso} of Eq. (39) and their derivatives satisfying Eqs. (42) and (44) are in the form

$$W_{\text{iso}}^{\text{inc}}\left(I_1,I_2,I_3\right)=\frac{A_1}{2}\left(I_1-3\right)+\frac{B_1}{2}\left(\frac{I_2}{I_3}-3\right), \tag{45}$$

$$\frac{\partial W_{\text{iso}}^{\text{inc}}}{\partial I_1}=\frac{A_1}{2},\ \frac{\partial W_{\text{iso}}^{\text{inc}}}{\partial I_2}=\frac{B_1}{2I_3},\ \frac{\partial W_{\text{iso}}^{\text{inc}}}{\partial I_3}=-\frac{B_1 I_2}{2I_3^2}, \tag{46}$$

$$W_{\text{iso}}^{\text{com}}\left(I_3\right)=\frac{C_1}{2}\left(\ln\sqrt{I_3}\right)^2-\left(A_1-B_1\right)\ln\sqrt{I_3}, \tag{47}$$

$$\frac{\partial W_{\text{iso}}^{\text{com}}}{\partial I_3}=\frac{C_1\ln I_3}{4I_3}-\frac{A_1-B_1}{2I_3}, \tag{48}$$

where A_1, B_1 and C_1 are material constants. The incompressible component $W_{\text{iso}}^{\text{inc}}$ and the compressible component $W_{\text{iso}}^{\text{com}}$ are the same as the strain energy function proposed by Attard [15] with $n=1$ ($L_1=I_1$ and $L^1=I_2/I_3$). The original generalized form in [15] is expressed as

$$W_{\text{iso}}^{\text{inc}} = \sum_{n=1}^{r} \frac{A_n}{2n}\left(L_n - 3\right) + \frac{B_n}{2n}\left(L^n - 3\right), \tag{49}$$

$$W_{\text{iso}}^{\text{comp}} = \sum_{n=1}^{s} \frac{C_n}{2n}\left(\ln\sqrt{I_3}\right)^{2n} - \left(\sum_{n=1}^{r} A_n - B_n\right)\ln\sqrt{I_3}. \tag{50}$$

$$L_n = \left(\lambda_{p1}\right)^{2n} + \left(\lambda_{p2}\right)^{2n} + \left(\lambda_{p3}\right)^{2n}, \tag{51}$$

$$L^n = \left(\lambda_{p1}\right)^{-2n} + \left(\lambda_{p2}\right)^{-2n} + \left(\lambda_{p3}\right)^{-2n}, \tag{52}$$

where $A_n, B_n \text{and } C_n$ are material constants, and L_n and L^n are invariants defined in terms of the principal stretches $\lambda_{pi}, i = 1, 2, 3$ as the equations above. $W_{\text{iso}}^{\text{inc}}$ is a incompressible component associated with constrained volume change or volume constant distortion and $W_{\text{iso}}^{\text{com}}$ is a compressible component associated with specific volume change. The incompressible component $W_{\text{iso}}^{\text{inc}}$ is the same as the generalized Mooney expression [16]. While the compressible component $W_{\text{iso}}^{\text{com}}$ is a generalization of the Simo and Pister proposal [17].

An advantage of this energy function which was successfully used for the analysis of isotropic hyperelastic materials [18, 19] is that the hydrostatic pressure component of the stress vector which is associated with volumetric dilation will have no shear component on any surface in any configuration.

3.1.2.2 Anisotropic strain energy function

For the anisotropic part W_{aniso} of Eq. (38), a generic form is considered and expressed as

$$W_{\text{aniso}}\left(I_3, J_{4i}, K_{5i}\right) = \sum_{r=1}^{m}\sum_{i=1}^{n} D^r\left[W_{\text{aniso}}^{Ir}\left(I_3\right) + W_{\text{aniso}}^{Jr}\left(J_{4i}\right) + W_{\text{aniso}}^{Kr}\left(K_{5i}\right)\right], \tag{53}$$

where D^r are material constants. The anisotropic part of the second Piola-Kirchhoff stress tensor are then given by

$$\boldsymbol{\pi}_{\text{aniso}} = 2\frac{\partial W_{\text{aniso}}}{\partial \mathbf{C}} \tag{54}$$

$$= 2\sum_{r=1}^{m}\sum_{i=1}^{n} D^r \left[\left(\frac{\partial W_{\text{aniso}}^{Ir}}{\partial I_3} I_3 + \frac{\partial W_{\text{aniso}}^{Kr}}{\partial K_{5i}} K_{5i} \right) \mathbf{C}^{-1} + \frac{\partial W_{\text{aniso}}^{Jr}}{\partial J_{4i}} \mathbf{G}_i - \frac{\partial W_{\text{aniso}}^{Kr}}{\partial K_{5i}} I_3 \mathbf{C}^{-1}\mathbf{G}_i\mathbf{C}^{-1} \right],$$

with $\partial I_3 / \partial \mathbf{C} = I_3\mathbf{C}^{-1}$, $\partial J_{4i} / \partial \mathbf{C} = \mathbf{G}_i$ and $\partial K_{5i} / \partial \mathbf{C} = K_{5i}\mathbf{C}^{-1} - I_3\mathbf{C}^{-1}\mathbf{G}_i\mathbf{C}^{-1}$.

The stress condition for the natural state is considered by setting $\mathbf{C} = \mathbf{I}$ and $\boldsymbol{\pi}_{\text{aniso}}\big|_{\mathbf{C}=\mathbf{I}} = \mathbf{0}$, i.e.,

$$\sum_{r=1}^{m}\sum_{i=1}^{n} D^r \left[\left(\frac{\partial W_{\text{aniso}}^{Ir}}{\partial I_3} + \frac{\partial W_{\text{aniso}}^{Kr}}{\partial K_{5i}} \right) \mathbf{I} + \left(\frac{\partial W_{\text{aniso}}^{Jr}}{\partial J_{4i}} - \frac{\partial W_{\text{aniso}}^{Kr}}{\partial K_{5i}} \right) \mathbf{G}_i \right] = \mathbf{0}, \tag{55}$$

with $I_1 = 3,\ I_2 = 3,\ I_3 = 1,$ and $J_{4i} = K_{5i} = \text{tr}\left[\mathbf{G}_i\right] = \mathbf{I}$ at $\mathbf{C} = \mathbf{I}$. Thus, the stress-free conditions are

$$\frac{\partial W_{\text{aniso}}^{Kr}(1)}{\partial K_{5i}} = \frac{\partial W_{\text{aniso}}^{Jr}(1)}{\partial J_{4i}} = -\frac{\partial W_{\text{aniso}}^{Ir}(1)}{\partial I_3} = 1, \quad r = 1, 2, ..., m, \quad i = 1, 2, ..., n. \tag{56}$$

For the energy-free reference configuration condition, $\mathbf{C} = \mathbf{I}$ is set and $W_{\text{aniso}}\big|_{\mathbf{C}=\mathbf{I}} = \mathbf{0}$ is required, i.e.,

$$\sum_{r=1}^{m}\sum_{i=1}^{n} D^r \left[W_{\text{aniso}}^{Ir}(1) + W_{\text{aniso}}^{Jr}(1) + W_{\text{aniso}}^{Kr}(1) \right] = 0. \tag{57}$$

Thus, the energy-free conditions are

$$W_{\text{aniso}}^{Ir}(1) = W_{\text{aniso}}^{Jr}(1) = W_{\text{aniso}}^{Kr}(1) = 0. \tag{58}$$

Some specific functions and their derivatives for the anisotropic part W_{aniso} of Eq. (53) which automatically satisfy Eqs. (56) and (58) are, e.g., the exponential functions of the form [20]

$$W_{\text{aniso}}^{Ir}(I_3) = \frac{1}{C_r}\left(I_3^{-C_r} - 1\right), \quad \frac{\partial W_{\text{aniso}}^{Ir}}{\partial I_3} = -I_3^{(-C_r - 1)},$$
$$W_{\text{aniso}}^{Jr}(J_{4i}) = \frac{1}{A_r}\left[e^{A_r(J_{4i}-1)} - 1\right], \quad \frac{\partial W_{\text{aniso}}^{Jr}}{\partial J_{4i}} = e^{A_r(J_{4i}-1)},$$
$$W_{\text{aniso}}^{Kr}(K_{5i}) = \frac{1}{B_r}\left[e^{B_r(K_{5i}-1)} - 1\right], \quad \frac{\partial W_{\text{aniso}}^{Kr}}{\partial K_{5i}} = e^{B_r(K_{5i}-1)}. \tag{59}$$

Alternatively, the logarithmic functions of the form

$$W_{\text{aniso}}^{Ir}(I_3) = \frac{1}{C_r}\left(I_3^{-C_r} - 1\right), \quad \frac{\partial W_{\text{aniso}}^{Ir}}{\partial I_3} = -I_3^{(-C_r - 1)},$$
$$W_{\text{aniso}}^{Jr}(J_{4i}) = -A_r \ln\left(1 - \frac{J_{4i}-1}{A_r}\right), \quad \frac{\partial W_{\text{aniso}}^{Jr}}{\partial J_{4i}} = \frac{A_r}{\left(A_r - J_{4i} + 1\right)},$$
$$W_{\text{aniso}}^{Kr}(K_{5i}) = -B_r \ln\left(1 - \frac{K_{5i}-1}{B_r}\right), \quad \frac{\partial W_{\text{aniso}}^{Kr}}{\partial K_{5i}} = \frac{B_r}{\left(B_r - K_{5i} + 1\right)}. \tag{60}$$

3.1.2.2.1 Anisotropic strain energy function for an incompressible material

With the incompressibility constraint $I_3 = 1$, the strain energy function W_{aniso} in Eq. (53) then becomes

$$W_{\text{aniso}}^{\text{inc}}\left(J_{4i}, K_{5i}^{\text{inc}}\right) = \sum_{r=1}^{m}\sum_{i=1}^{n} D^r\left[W_{\text{aniso}}^{Jr}\left(J_{4i}\right) + W_{\text{aniso}}^{Kr}\left(K_{5i}^{\text{inc}}\right)\right], \tag{61}$$

$$K_{5i}^{\text{inc}} = \text{tr}\left[\mathbf{C}^{-1}\mathbf{G}_i\right], \tag{62}$$

where K_{5i}^{inc} are the invariants K_{5i} under the incompressibility constraint $I_3 = 1$.

3.2 Validation

In this section, the proposed formulation Eq. (38) is validated and verified by comparing the results with available experimental and numerical results.

Soft biological tissues are the materials that can exhibit different mechanical characteristics due to their complex structures. The main part of tissue that usually provides structural support for cells is the extracellular matrix which composes of the collagen, elastin and ground substance. The collagen forms fibers or networks providing reinforcing structures. The elastin gives stiffness to the tissue and stores most of the strain energy at small strains while at large strains, collagen fibers play an important role. With increasing deformation these fibers produce a strong growth in tissue stiffness. This type of matemial can thus undergo large nonlinear elastic deformations and have high anisotropic characteristics [21].

The model is specified and applied to predicting the large nonlinear elastic behavior in soft biological tissues under uniaxial and biaxial states of stress. In order to describe the mechanical behavior of the tissue samples, an incompressible fiber-reinforced composite is often assumed for each layer with two mechanically equivalent families of collagen fibers that form symmetrical helices tilted by an angle $\pm\varphi$ against the circumferential direction [22, 23]. This assumption is also adopted in this study.

3.2.1 Uniaxial tension tests on arterial tissue

The proposed model is applied to a set of experimental data on human arterial tissue performed by Holzapfel et al. [24]. Arteries were split into the adventitial, medial and intimal layer and tested in cyclic uniaxial quasi-static tension. The load was applied such that the principal axes of deformation coincided with the circumferential, axial and radial direction of the vessel. The stress response for loading in circumferential and axial direction was recorded.

In order to describe the mechanical behavior of the tissue samples, the mentioned assumption of considering each layer as an incompressible fiber-reinforced material with two equivalent families of fibers arranged by an angle $\pm\varphi$ is adopted. For the isotropic term, Eq. (45) is adopted while Eq. (61) is utilized for the anisotropic term with Eq. (59) as a clearly exponential shape of the test results is observed. The orientations of the two fiber families can be given by the vectors

$$\mathbf{m}_1 = \cos\varphi\mathbf{e}_\theta + \sin\varphi\mathbf{e}_z, \quad \mathbf{m}_2 = \cos\varphi\mathbf{e}_\theta - \sin\varphi\mathbf{e}_z, \tag{63}$$

where $\mathbf{e}_\theta$ and $\mathbf{e}_z$ are unit vectors in the circumferential and axial direction of the artery, respectively. Applying Eqs. (22), (25) and (62), the two generalized invariants can be expressed in terms of the principal stretches under the incompressibility constraint $I_3 = \lambda_\theta\lambda_z\lambda_r = 1$ as

$$\begin{aligned} J_{4i} &= \lambda_\theta^2 \cos^2\varphi + \lambda_z^2 \sin^2\varphi, \\ K_{5i}^{\text{inc}} &= \lambda_\theta^{-2} \cos^2\varphi + \lambda_z^{-2} \sin^2\varphi, \end{aligned} \tag{64}$$

where λ_θ, λ_z and λ_r are the principal stretches in circumferential, axial and radial direction, respectively. Considering one single term m = 1 and n = 2 with taking into account the mechanical equivalence of the fiber families, so that $w_2^1 = w_1^1,\ J_{42} = J_{41}$ and $K_{52}^{\text{inc}} = K_{51}^{\text{inc}}$, the strain energy function Eq. (38) for an incompressible material with the exponential functions is then given by

$$W = \left(1-2w_1^1\right)\left[\frac{A_1}{2}\left(I_1-3\right)+\frac{B_1}{2}\left(\frac{I_2}{I_3}-3\right)\right] \\ +2w_1^1D^1\left[\frac{1}{A_1}\left(e^{A_1\left(J_{41}-1\right)}-1\right)+\frac{1}{B_1}\left(e^{B_1\left(K_{51}^{\text{inc}}-1\right)}-1\right)\right]. \tag{65}$$

For uniaxial tension test, the lateral directions are stress free and the Cauchy stresses in circumferential and axial direction can be calculated, respectively, by

$$\sigma_\theta = \lambda_\theta \frac{\partial W}{\partial \lambda_\theta}, \qquad \sigma_z = \lambda_z \frac{\partial W}{\partial \lambda_z}. \tag{66}$$

Fig. 3 shows the comparison results as Cauchy stress versus stretch diagrams. The proposed model was fitted and compared to the experimental results as well as the prediction results of Ehret and Itskov [23]. The five model parameters (A_1, B_1, D_1, w_1^1 and φ) for each layer, i.e. intimal, medial and adventitial layer, were determined by using a least squares regression analysis of the experimental data implemented using the commercial package MATLAB. The values of the parameters as well as the sum squared error (SSE) and R-square (R^2) obtained from the fittings are also presented in Fig. 3.

For all three layers, i.e. intimal layer in Fig. 3(a), medial layer in Fig. 3(b) and adventitial layer Fig. 3(c), the comparisons are in good agreement with the experiemental results with R^2 of 0.9978, 0.9995 and 0.9981, respectively.

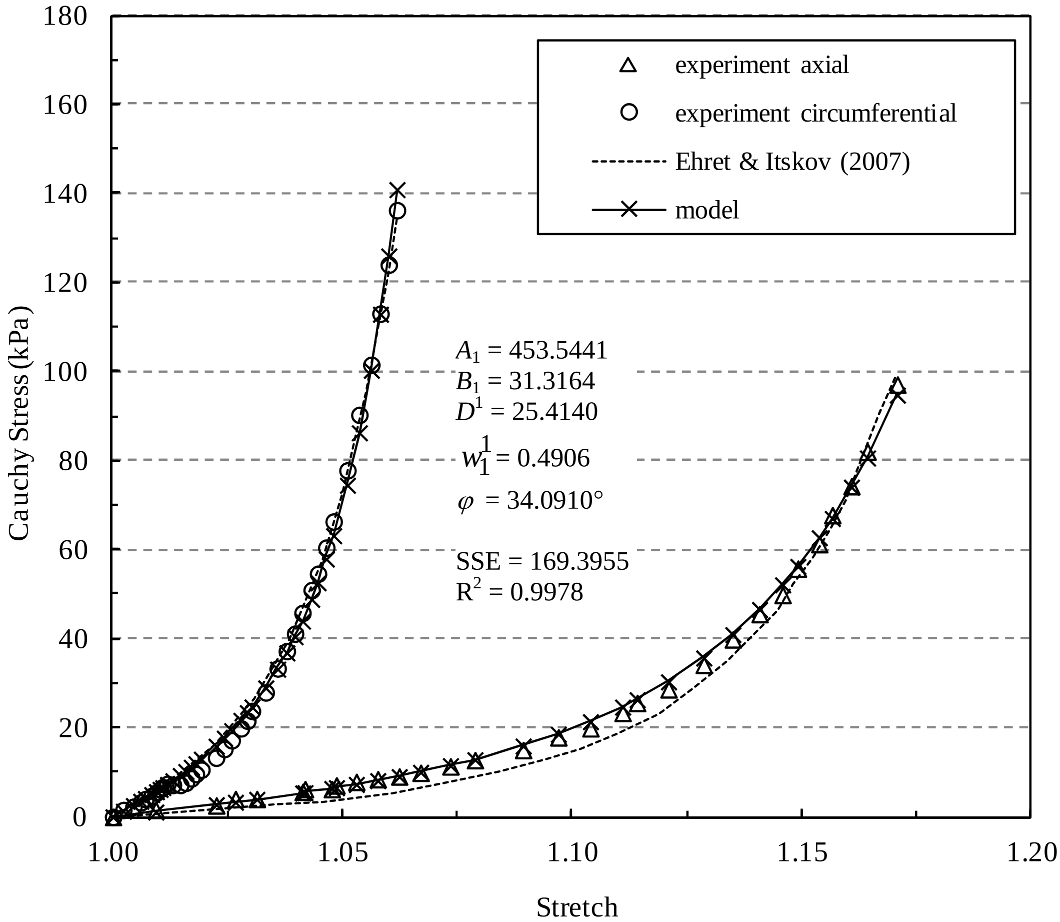

(a) Intima layer

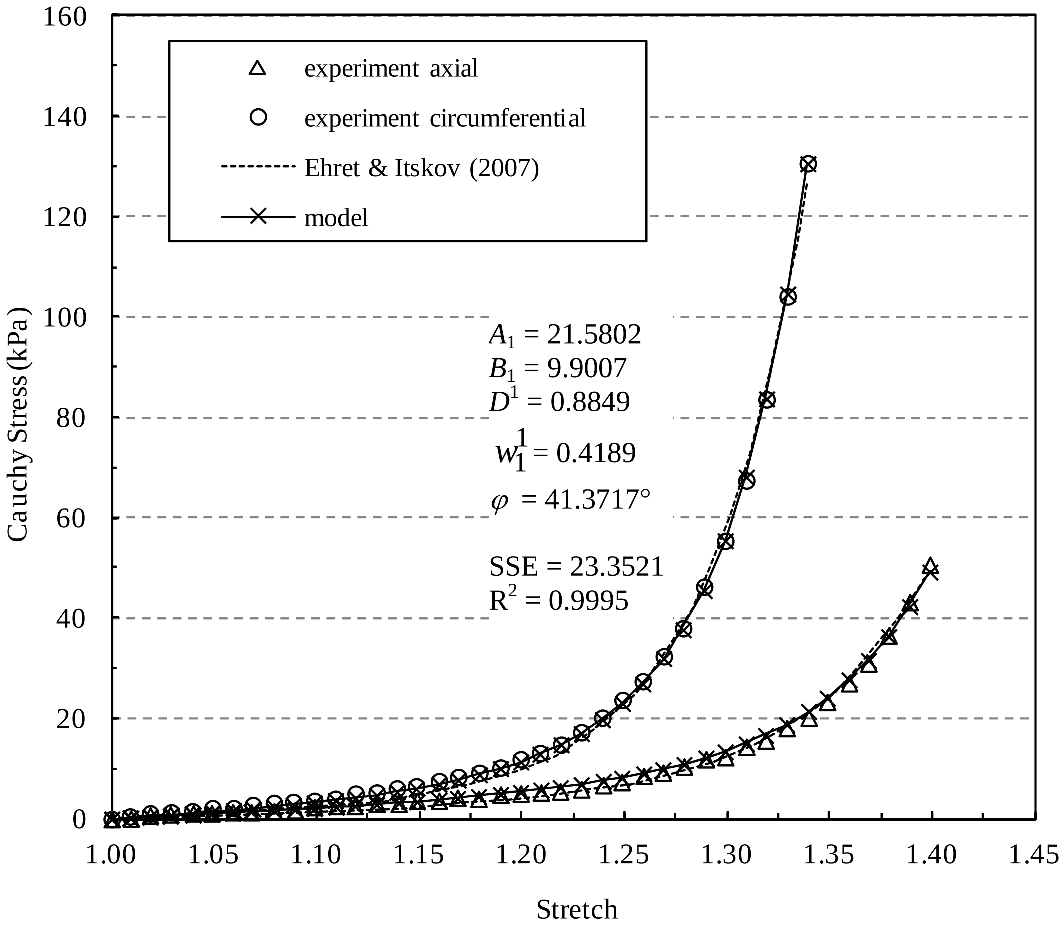

(b) Media layer

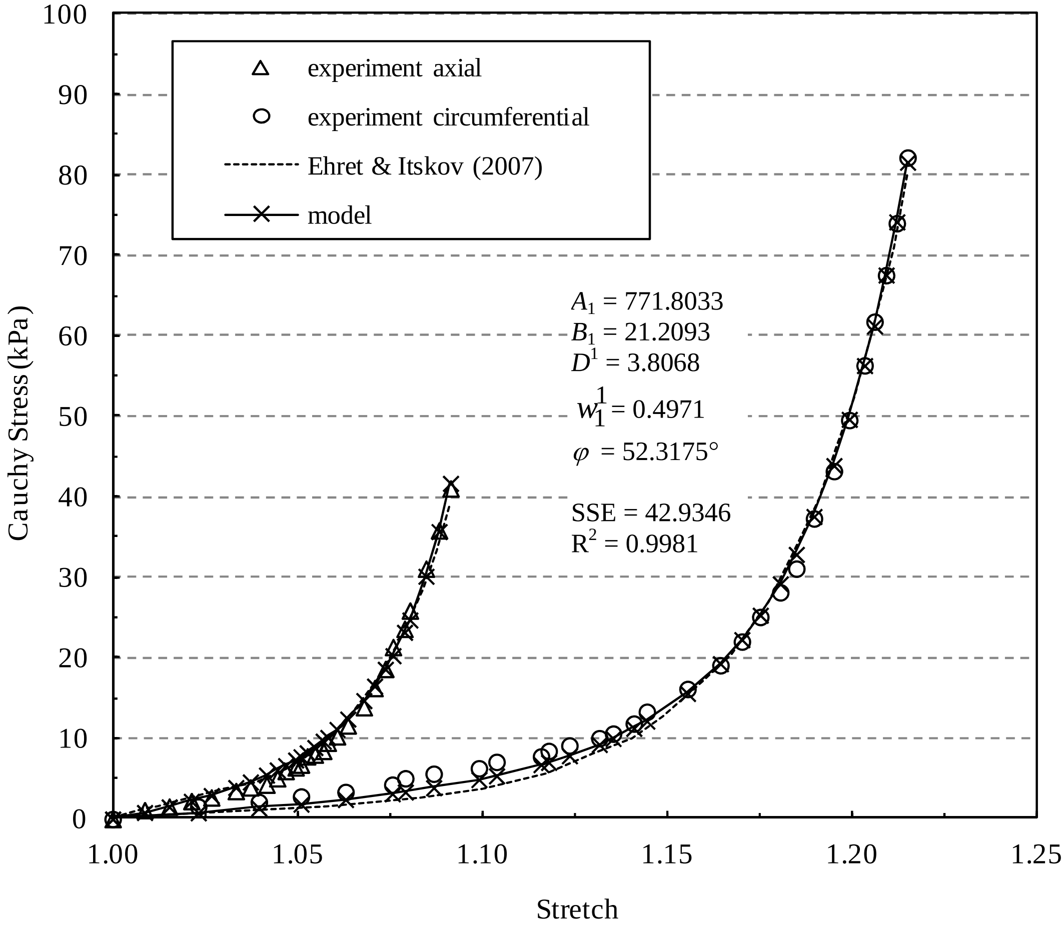

(c) Adventitia layer

Fig. 3 Comparisons of the model results with the experimental results under uniaxial tension tests and with the prediction results of Ehret and Itskov [23]

3.2.2 Biaxial tension tests on abdominal aorta

In this validation, the proposed model is applied to prediction of the anisotropic behavior in human abdominal aorta under biaxial state of stress carried out by Geest et al. [25] to study the age dependency of the behavior. The square samples were biaxially loaded in circumferential and axial direction with different ratios between circumferential and axial tension, $p_{\theta\theta} : p_{zz}$. It was reported that the stress responses of samples obtained from different age groups had different shapes. The stress-strain curves in terms of the second Piola-Kirchhoff stress and the Green-Lagrange strain changed from a sigmoidal shape in the youngest group (< 30 years) to an exponential nature in the older ones.

To model the stress response of the young arteries, the whole artery is considered as an incompressible fiber-reinforced material with two symmetrically arranged fiber helices and thus assumed that the principal axis of deformation coincide with the circumferential, axial and radial direction [23]. The fiber orientation in Eq. (63) and the generalized invariants in Eq. (64) are used. For the strain energy function, Eq. (45) is still adopted for the isotropic part but the logarithmic form of Eq. (60) is utilized for the anisotropic part due to the s-shaped stress-strain curves observed. By setting m = 1 and n = 2 as well as taking into account the mechanical equivalence of the fiber families, the strain energy function Eq. (38) for an incompressible material with the logarithmic functions is then given by

$$\begin{aligned} W = &\left(1-2w_1^1\right)\left[\frac{A_1}{2}\left(I_1-3\right)+\frac{B_1}{2}\left(\frac{I_2}{I_3}-3\right)\right] \\ &+2w_1^1 D^1\left[-A_1 \ln\left(1-\frac{J_{41}-1}{A_1}\right)-B_1 \ln\left(1-\frac{K_{51}^{\mathrm{inc}}-1}{B_1}\right)\right]. \end{aligned} \tag{67}$$

For biaxial tension test, the radial direction is stress free. The second Piola-Kirchhoff stresses in circumferential and axial direction can be calculated, respectively, by

$$\pi_\theta = \lambda_\theta^{-1}\frac{\partial W}{\partial \lambda_\theta}, \qquad \pi_z = \lambda_z^{-1}\frac{\partial W}{\partial \lambda_z}. \tag{68}$$

The proposed model was first fitted to the experimental results (specimen 3 in [25]) with $p_{\theta\theta} : p_{zz}$ ratios of 0.5:1, 1:1 and 1:0.5. The comparison results are presented in Fig. 4. The obtained model parameters were then used to predict the remaining test results with $p_{\theta\theta} : p_{zz}$ ratios of 0.75:1 and 1:0.75 as depicted in Fig. 5. A good agreement with the experimental results shows in Fig. 4 with R^2 = 0.9830 and in Fig. 5 with R^2 = 0.9888.

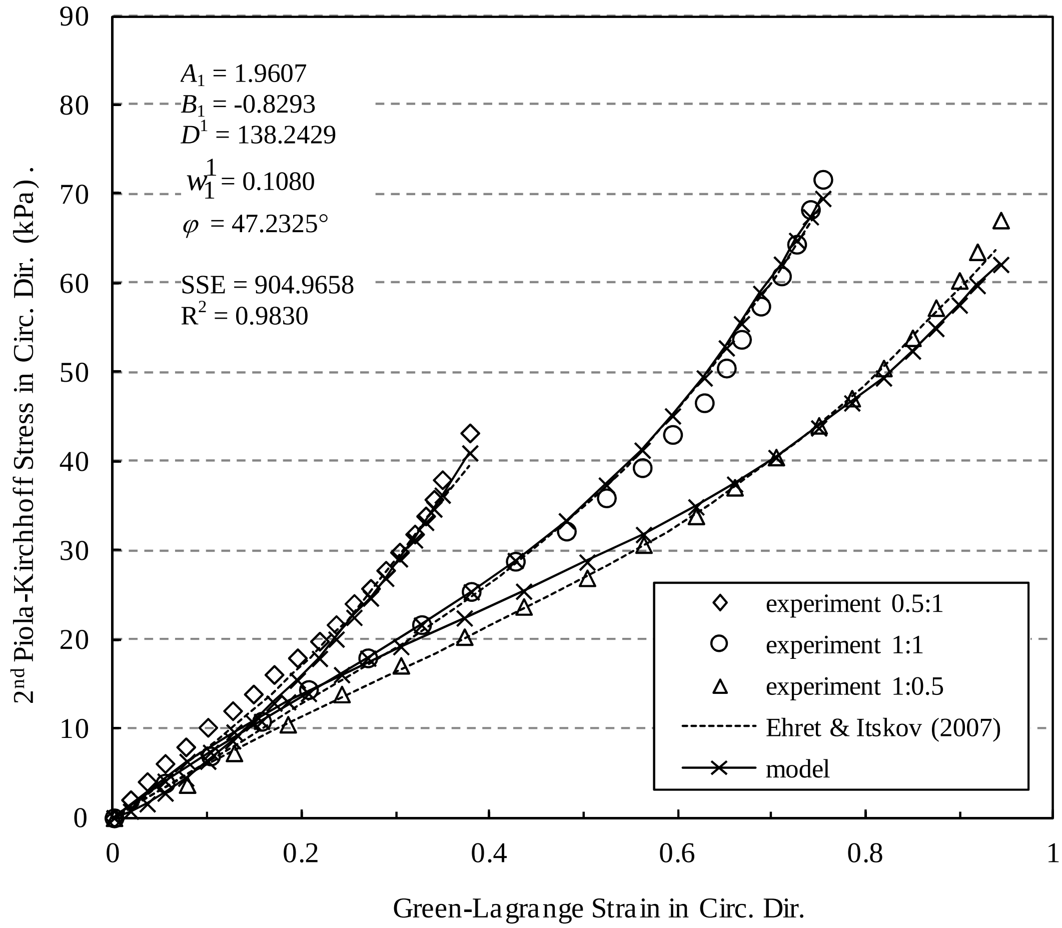

(a) In circumferential direction

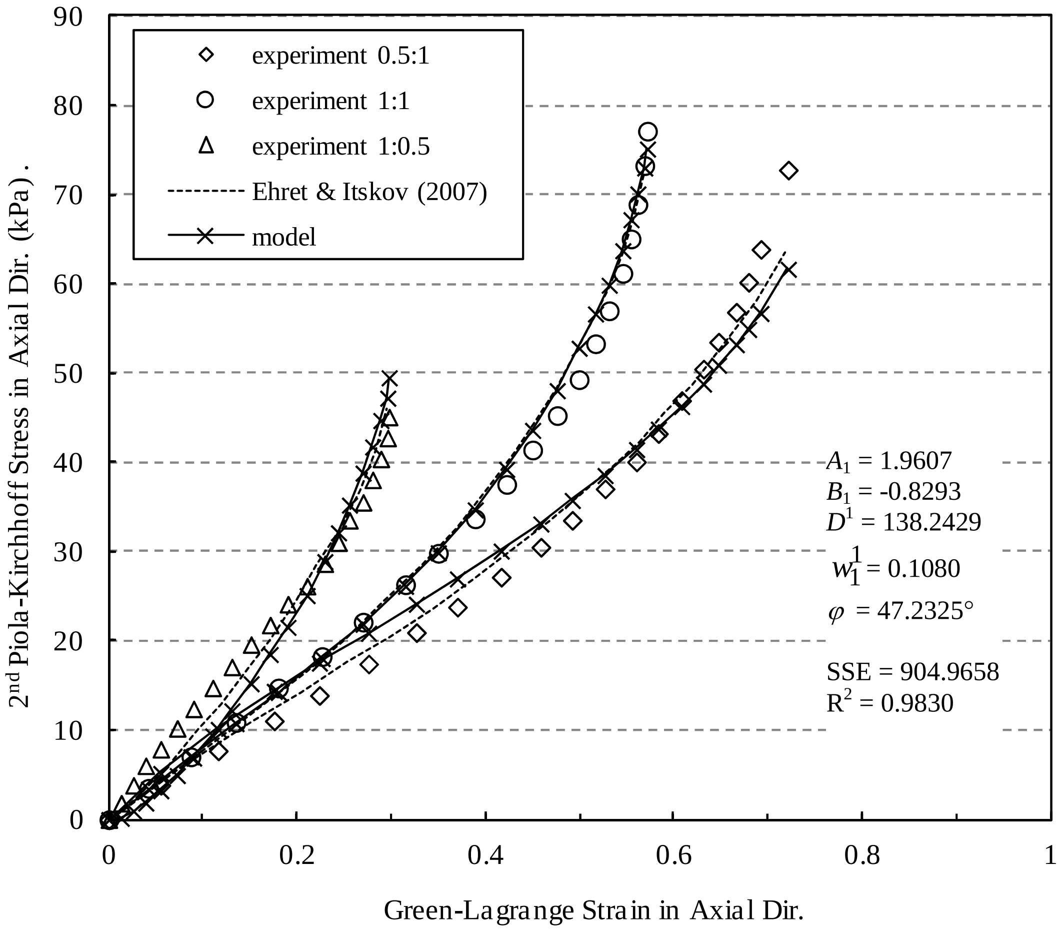

(b) In axial direction

Fig. 4 Comparisons of the model results with the prediction results of Ehret and Itskov [23] and with the experimental results under biaxial tension tests with $p_{\theta\theta} : p_{zz}$ ratios of 0.5:1, 1:1 and 1:0.5

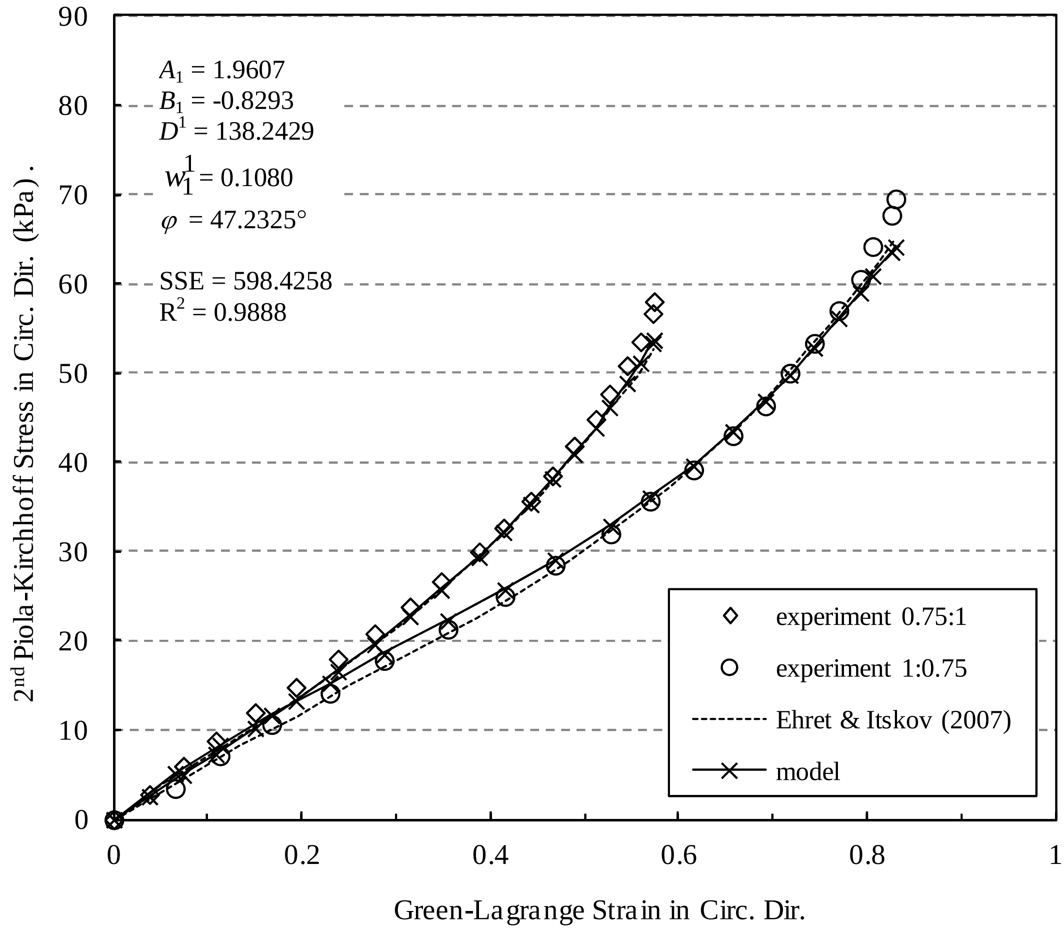

(a) In circumferential direction

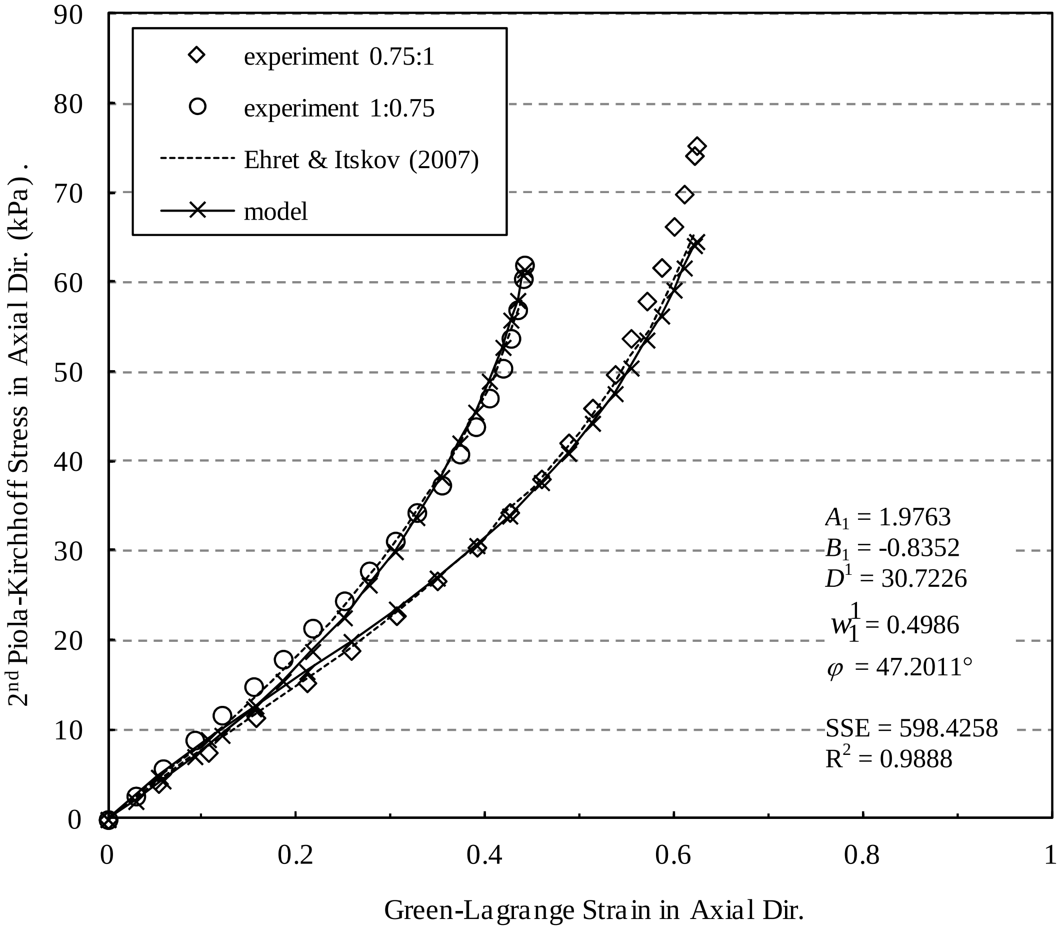

(b) In axial direction

Fig. 5 Comparisons of the model results with the prediction results of Ehret and Itskov [23] and with the experimental results under biaxial tension tests with $p_{\theta\theta} : p_{zz}$ ratios of 0.75:1 and 1:0.75

Chapter 4

Hyperelastic Formulation of Column Buckling Equation

In Chapter 3, the strain energy functions for anisotropic hyperelastic materials under finite strain have been derived. In this chapter, anisotropic constitutive relationships using the developed strain energy functions are established for determining buckling equations which include shear deformations for anisotropic columns.

4.1 Hyperelastic Constitutive Modeling

According to the proposed strain energy function in Eq. (38), a simple form, for the isotropic part W_{iso} and for the anisotropic part W_{aniso}, is considered for this purpose. The constitutive modeling for isotropic materials proposed by [3] is recapitulated and adopted herein.

4.1.1 Constitutive Modeling for Isotropic Part

A simple form, the neo-Hookean constitutive relationship, for the isotropic part of the strain energy function is adopted herein as (see [3])

$$W_{\text{iso}} = \frac{A_1}{2}\left\{tr\left(\mathbf{C}-\mathbf{I}\right)-2\ln J\right\}+\frac{C_1}{2}\left(\ln J\right)^2, \tag{69}$$

where, for isotropic materials, A_1 = the shear modulus $G=\frac{E}{2(1+\nu)}$, C_1 = the Lame constant $\Lambda=\frac{2G\nu}{(1-2\nu)}$, E is the elastic modulus and ν is the Poisson's ratio. Therefore, the second Piola Kirchhoff stress tensor for the isotropic part $\mathbf{\Pi}_{iso}$ can be expressed as

$$\mathbf{\Pi}_{iso} = 2\frac{\partial W_{iso}}{\partial \mathbf{C}} = A_1\left[\mathbf{I}-\mathbf{C}^{-1}\right]+C_1\ln J\mathbf{C}^{-1} = A_1\mathbf{I}-p_h\mathbf{C}^{-1}, \tag{70}$$

where $p_h = A_1 - C_1\ln J$ represents a hydrostatic stress. The Mandel stress tensor for the isotropic part $\mathbf{M}_{iso}$, which is another Langrangian stress tensor, is defined by

$$\mathbf{M}_{iso} = \mathbf{C}\mathbf{\Pi}_{iso} \tag{71}$$

Using Eq. (70), the Mandel stress tensor is given by

$$\mathbf{M}_{iso} = \mathbf{M}_{iso}^{T} = A_1\mathbf{C} - p_h\mathbf{I}. \tag{72}$$

The Mandel stress tensor, which is not generally symmetric, is found to be symmetric with the expression above. Substituting Eq. (12) into Eq. (72), the Mandel stress tensor components can be written as

$$\mathbf{M}_{iso} = \begin{bmatrix} A_1(\lambda_1)^2 - p_h & A_1\lambda_1\lambda_2\cos\varphi_{12} & A_1\lambda_1\lambda_3\cos\varphi_{13} \\ A_1\lambda_1\lambda_2\cos\varphi_{12} & A_1(\lambda_2)^2 - p_h & A_1\lambda_2\lambda_3\cos\varphi_{23} \\ A_1\lambda_1\lambda_3\cos\varphi_{13} & A_1\lambda_2\lambda_3\cos\varphi_{23} & A_1(\lambda_3)^2 - p_h \end{bmatrix}. \tag{73}$$

4.1.2 Constitutive Modeling for Anisotropic Part

A simple form for the anisotropic part of the strain energy function is adopted herein as

$$W_{\text{aniso}} = D^1\left[\frac{1}{B_1}\left(e^{B_1(K_{51}-1)} - 1\right)\right]. \tag{74}$$

Therefore, the second Piola Kirchhoff stress tensor for the anisotropic part $\mathbf{\Pi}_{aniso}$ can be written as

$$\mathbf{\Pi}_{aniso} = 2\frac{\partial W_{aniso}}{\partial \mathbf{C}} = 2D^1 e^{B_1(K_{51}-1)}\left(K_{51}\mathbf{C}^{-1} - I_3\mathbf{C}^{-1}G_1\mathbf{C}^{-1}\right). \tag{75}$$

Using Eq. (75), the Mandel stress tensor for the anisotropic part $\mathbf{M}_{aniso}$ is given by

$$\begin{aligned}
&\mathbf{M}_{aniso} = \mathbf{M}_{aniso}^{T} = \mathbf{C}\mathbf{\Pi}_{aniso} = 2D^1 e^{B_1(K_{51}-1)}\left(K_{51}\mathbf{I} - I_3\mathbf{C}^{-1}G_1\right), \\
&\mathbf{M}_{aniso}^{11} = 2D^1 e^{B_1(K_{51}-1)}\left\{K_{51} - G_1(\lambda_2)^2(\lambda_3)^2\right\}, \\
&\mathbf{M}_{aniso}^{12} = \mathbf{M}_{aniso}^{21} = 2D^1 e^{B_1(K_{51}-1)}\left\{G_1\lambda_1\lambda_2(\lambda_3)^2\cos\varphi_{12}\right\}, \\
&\mathbf{M}_{aniso}^{13} = \mathbf{M}_{aniso}^{31} = 2D^1 e^{B_1(K_{51}-1)}\left\{G_1\lambda_1(\lambda_2)^2\lambda_3\cos\varphi_{13}\right\}, \\
&\mathbf{M}_{aniso}^{22} = 2D^1 e^{B_1(K_{51}-1)}\left\{K_{51} - G_1(\lambda_1)^2(\lambda_3)^2\left(1-\cos^2\varphi_{13}\right)\right\}, \\
&\mathbf{M}_{aniso}^{23} = \mathbf{M}_{aniso}^{32} = -2D^1 e^{B_1(K_{51}-1)}\left\{G_1(\lambda_1)^2\lambda_2\lambda_3\cos\varphi_{12}\cos\varphi_{13}\right\}, \\
&\mathbf{M}_{aniso}^{33} = 2D^1 e^{B_1(K_{51}-1)}\left\{K_{51} - G_1(\lambda_1)^2(\lambda_2)^2\left(1-\cos^2\varphi_{12}\right)\right\}.
\end{aligned} \tag{76}$$

4.2 Equilibrium and Virtual Work

Assuming all external loading is conservative, the system is static and all body forces are zero, the equilibrium equations at a point within a continuum can be expressed as (see [3])

$$\nabla \cdot \left(\mathbf{\Pi F}^T \right) = \nabla \cdot \mathbf{S} = \mathbf{0}, \qquad \left[\Pi^{ir} \left(\delta_r^j + u^j \Big|_r \right) \right] \Bigg|_i = S^{ij} \Big|_i = 0, \tag{77}$$

where $\mathbf{S}$ is the first Piola Kirchhoff stress tensor. The moment equilibrium, which must also be satisfied, are

$$\mathbf{\Pi}^T = \mathbf{\Pi}, \qquad \mathbf{FS} = \mathbf{S}^T \mathbf{F}^T. \tag{78}$$

The following must also be satisfied at the loaded boundary surfaces

$$\mathbf{n} \cdot \left(\mathbf{\Pi F}^T \right) = \mathbf{n} \cdot \mathbf{S} = \mathbf{p}, \qquad \Pi^{ir} \left(\delta_r^j + u^j \Big|_r \right) n_i = S^{ij} n_i = p^j, \tag{79}$$

where n_i are the covariant components of the unit normal vector $\mathbf{n}$ to the boundary surfaces and p^j are the contravariant vector components of the applied surface tractions $\mathbf{p}$ with respect to the undeformed state.

Using the theorem of virtual work, the equilibrium equations can also be expressed in a weaker form. For kinematically admissible variation δ, the Lagrangain first variation of work δU based on virtual displacements can be expressed as

$$\delta U = \iiint_V \delta W dV - \iint_S \mathbf{p} \cdot \delta \mathbf{u} dS = \iiint_V \frac{1}{2} tr \left(\mathbf{\Pi} \delta \mathbf{C} \right) dV - \iint_S \mathbf{p} \cdot \delta \mathbf{u} dS = 0, \tag{80}$$

where V is the volume in the undeformed state, S is the surface where the traction vector $\mathbf{p}$ acts. Substituting Eq. (12) into Eq. (80), the first variation of work becomes

$$\delta U=\iiint_V\begin{bmatrix}\left\{\Pi^{11}\lambda_1+\Pi^{12}\lambda_2\cos\varphi_{12}+\Pi^{13}\lambda_3\cos\varphi_{13}\right\}\delta\lambda_1\\+\left\{\Pi^{22}\lambda_2+\Pi^{12}\lambda_1\cos\varphi_{12}+\Pi^{23}\lambda_3\cos\varphi_{23}\right\}\delta\lambda_2\\+\left\{\Pi^{33}\lambda_3+\Pi^{13}\lambda_1\cos\varphi_{13}+\Pi^{23}\lambda_2\cos\varphi_{23}\right\}\delta\lambda_3\\-\Pi^{12}\lambda_1\lambda_2\sin\varphi_{12}\delta\varphi_{12}-\Pi^{13}\lambda_1\lambda_3\sin\varphi_{13}\delta\varphi_{13}-\Pi^{23}\lambda_2\lambda_3\sin\varphi_{23}\delta\varphi_{23}\end{bmatrix}dV$$
$$-\iint_S\mathbf{p}\cdot\delta\mathbf{u}dS=0. \tag{81}$$

4.3 Large Deformation Uniaxial Beam Plane Stress

For the plane stress case and uniaxial deformation as in thick beam bending, the virtual work terms with respect to $\delta\lambda_2,\delta\lambda_3\ \&\ \delta\varphi_{23}$ would be zero (see [3]).

From Eq. (81), the stress terms

$$\begin{gathered}\Pi^{22}\lambda_2+\Pi^{12}\lambda_1\cos\varphi_{12}+\Pi^{23}\lambda_3\cos\varphi_{23}\\\Pi^{33}\lambda_3+\Pi^{13}\lambda_1\cos\varphi_{13}+\Pi^{23}\lambda_2\cos\varphi_{23},\end{gathered} \tag{82}$$

are the physical Lagrangain stresses conjugate to the stretch variations $\delta\lambda_2\ \&\ \delta\lambda_3$, respectively.

4.3.1 For Isotropic Part

Assuming $\varphi_{23}=\frac{\pi}{2}$ and using the constitutive relationship Eq. (73), it can be shown that the stresses in Eq. (82) are zero if

$$\left(\lambda_2\right)_{iso}=\sqrt{\frac{p_h}{A_1}},\quad\left(\lambda_3\right)_{iso}=\sqrt{\frac{p_h}{A_1}}. \tag{83}$$

Therefore, substituting Eq. (83) and $\varphi_{23}=\frac{\pi}{2}$ into Eq. (81), the virtual work for plane stress is given by

$$\delta U_{iso}=\iiint_V\begin{bmatrix}\left\{\Pi^{11}\lambda_1+\sqrt{\frac{p_h}{A_1}}\left(\Pi^{12}\cos\varphi_{12}+\Pi^{13}\cos\varphi_{13}\right)\right\}\delta\lambda_1\\-\lambda_1\sqrt{\frac{p_h}{A_1}}\left(\Pi^{12}\sin\varphi_{12}\delta\varphi_{12}-\Pi^{13}\sin\varphi_{13}\delta\varphi_{13}\right)\end{bmatrix}dV-\iint_S\mathbf{p}\cdot\delta\mathbf{u}dS=0. \tag{84}$$

And substituting Eq. (83) and $\varphi_{23}=\frac{\pi}{2}$ into Eq. (73), the state of stress for plane stress for large deformations is given by

$$\mathbf{M}_{iso}=\begin{bmatrix} A_1(\lambda_1)^2-p_h & A_1\lambda_1\sqrt{\frac{p_h}{A_1}}\cos\varphi_{12} & A_1\lambda_1\sqrt{\frac{p_h}{A_1}}\cos\varphi_{13} \\ A_1\lambda_1\sqrt{\frac{p_h}{A_1}}\cos\varphi_{12} & 0 & 0 \\ A_1\lambda_1\lambda_3\cos\varphi_{13} & 0 & 0 \end{bmatrix}. \tag{85}$$

4.3.2 For Anisotropic Part

Similarly, assuming $\varphi_{23}=\frac{\pi}{2}$ and using the constitutive relationship Eq. (76), it can be shown that the stresses in Eq. (82) are zero if

$$(\lambda_2)_{aniso}=\frac{1}{\lambda_1}\sqrt{\frac{K_{51}}{G_1\left(1-\cos^2\varphi_{12}\right)}},\quad (\lambda_3)_{aniso}=\frac{1}{\lambda_1}\sqrt{\frac{K_{51}}{G_1\left(1-\cos^2\varphi_{13}\right)}}. \tag{86}$$

Hence, substituting Eq. (86) and $\varphi_{23}=\frac{\pi}{2}$ into Eq. (81), the virtual work for plane stress becomes

$$\begin{aligned}\delta U_{aniso}=&\iiint_V\begin{bmatrix}\left\{\Pi^{11}\lambda_1+\Pi^{12}(\lambda_2)_{aniso}\cos\varphi_{12}+\Pi^{13}(\lambda_3)_{aniso}\cos\varphi_{13}\right\}\delta\lambda_1\\ -\Pi^{12}\lambda_1(\lambda_2)_{aniso}\sin\varphi_{12}\delta\varphi_{12}-\Pi^{13}\lambda_1(\lambda_3)_{aniso}\sin\varphi_{13}\delta\varphi_{13}\end{bmatrix}dV\\ &-\iint_S\mathbf{p}\cdot\delta\mathbf{u}dS \end{aligned} \tag{87}$$

$$\begin{aligned}=&\iiint_V\begin{bmatrix}\left\{\begin{matrix}\Pi^{11}\lambda_1+\Pi^{12}\dfrac{1}{\lambda_1}\sqrt{\dfrac{K_{51}}{G_1\left(1-\cos^2\varphi_{12}\right)}}\cos\varphi_{12}\\ +\Pi^{13}\dfrac{1}{\lambda_1}\sqrt{\dfrac{K_{51}}{G_1\left(1-\cos^2\varphi_{13}\right)}}\cos\varphi_{13}\end{matrix}\right\}\delta\lambda_1\\ -\Pi^{12}\sqrt{\dfrac{K_{51}}{G_1\left(1-\cos^2\varphi_{12}\right)}}\sin\varphi_{12}\delta\varphi_{12}\\ -\Pi^{13}\sqrt{\dfrac{K_{51}}{G_1\left(1-\cos^2\varphi_{13}\right)}}\sin\varphi_{13}\delta\varphi_{13}\end{bmatrix}dV\\ &-\iint_S\mathbf{p}\cdot\delta\mathbf{u}dS=0.\end{aligned}$$

And substituting Eq. (86) and $\varphi_{23}=\frac{\pi}{2}$ into Eq. (76), the state of stress for plane stress for large deformations becomes

$$\mathbf{M}^{11}_{aniso} = -2D^1 e^{B_1(K_{51}-1)} \left\{ \frac{K_{51}^2}{G_1(\lambda_1)^4(1-\cos^2\varphi_{13})(1-\cos^2\varphi_{12})} - K_{51} \right\},$$
$$\mathbf{M}^{12}_{aniso} = \mathbf{M}^{21}_{aniso} = \frac{2D^1 e^{B_1(K_{51}-1)} \left\{ K_{51}\cos\varphi_{12}\sqrt{K_{51}} \right\}}{(\lambda_1)^2(1-\cos^2\varphi_{13})\sqrt{G_1(1-\cos^2\varphi_{12})}},$$
$$\mathbf{M}^{13}_{aniso} = \mathbf{M}^{31}_{aniso} = \frac{2D^1 e^{B_1(K_{51}-1)} \left\{ K_{51}\cos\varphi_{13}\sqrt{K_{51}} \right\}}{(\lambda_1)^2(1-\cos^2\varphi_{12})\sqrt{G_1(1-\cos^2\varphi_{13})}},$$
$$\mathbf{M}^{22}_{aniso} = 0,$$
$$\mathbf{M}^{23}_{aniso} = \mathbf{M}^{32}_{aniso} = \frac{-2D^1 e^{B_1(K_{51}-1)} \left\{ K_{51}\cos\varphi_{12}\cos\varphi_{13} \right\}}{\sqrt{(1-\cos^2\varphi_{12})(1-\cos^2\varphi_{13})}},$$
$$\mathbf{M}^{33}_{aniso} = 0. \tag{88}$$

4.4 Beam Bending with Shear – Timoshenko Beam

In this section, a straight prismatic beam is considered as a three-dimensional problem with bending, shear and axial deformation (see [3]).

The longitudinal axis of centroids of the undeformed beam is taken as the x or 1 axis (see Fig. 6). The y or 2 axis and the z or 3 axis are taken as the principal axes in the plane of the cross-section.

The deflection of the centroidal axis and the rotation of the cross-sectional plane are assumed to govern the deflected shape of the beam. The Timoshenko beam approximation is adopted as during deformation, it is assumed that the plane of the cross-section remains plane but not perpendicular to the centroidal axis. In the deformed state, the angle between the material base vector $\hat{\mathbf{g}}_1$ and the undeformed longitudinal axis consists of a bending component θ and shear components described by the angles $\varphi \,\&\, \alpha$. The tangent base vectors $\hat{\mathbf{g}}_2$ and $\hat{\mathbf{g}}_3$ are assumed to remain orthogonal or $\hat{\mathbf{g}}_2 \cdot \hat{\mathbf{g}}_3 = 0$. The unit vector $\hat{\mathbf{n}}$, which is defined by $\hat{\mathbf{g}}_2 \times \hat{\mathbf{g}}_3$ and normal to the cross-sectional plane in the deformed state, lies in the plane of $\mathbf{g}_1$ and $\mathbf{g}_2$ and is given by

$$\hat{\mathbf{n}} = \cos\theta\mathbf{i}_1 + \sin\theta\mathbf{i}_2, \quad \hat{\mathbf{t}} = -\sin\theta\mathbf{i}_1 + \cos\theta\mathbf{i}_2, \quad \hat{\mathbf{b}} = \mathbf{i}_3 \tag{89}$$

where $\mathbf{i}_1, \mathbf{i}_2$ and $\mathbf{i}_3$ are unit base vectors in the x, y and z directions, respectively. The unit vectors $\hat{\mathbf{n}}, \hat{\mathbf{t}} \,\&\, \hat{\mathbf{b}}$ form an orthonormal set. The angle ϕ defines the rotation or torsion of the $\hat{\mathbf{g}}_2$ & $\hat{\mathbf{g}}_3$ axes about the unit vector $\hat{\mathbf{n}}$.

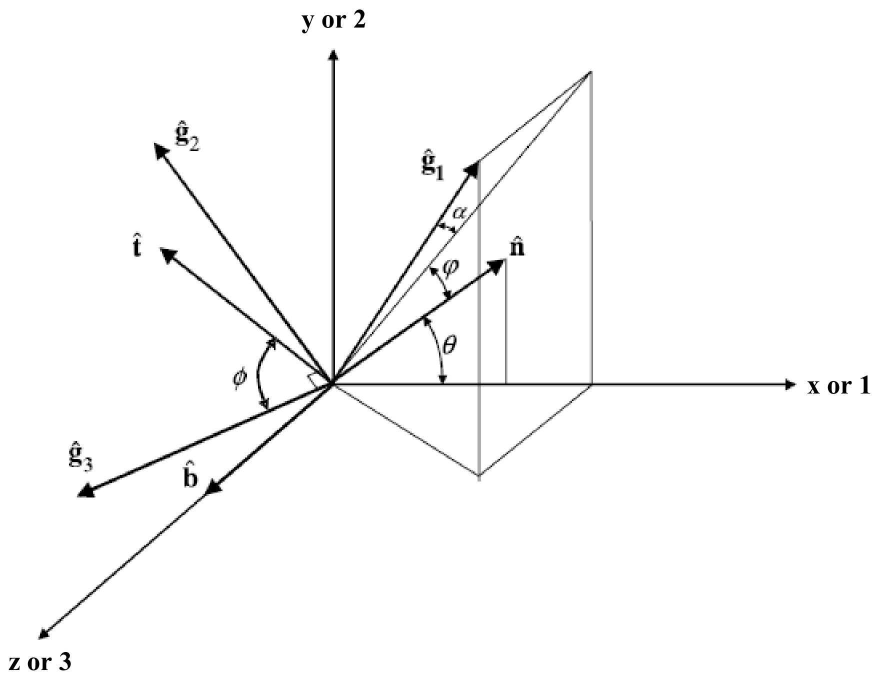

Fig. 6 Tangent base vectors in the deformed state [3]

The bending angle is assumed to be a function of x only, $\theta = \theta$(x), while the shear angles $\varphi \,\&\, \alpha$ are taken as a function of the coordinates x, y and z. At the level of the centroid (y and z = 0), the shear angles are assumed as

$$\varphi(x,0,0) = \varphi_0, \quad \alpha(x,0,0) = 0. \tag{90}$$

The condition of $\hat{\mathbf{g}}_2 \cdot \hat{\mathbf{g}}_3 = 0$ and the conditions mentioned in Eq. (83) for isotropic part or in Eq. (86) for anisotropic part are utilised to allow for unrestrained dilation so that the stress state in bending is approximately uniaxial. The tangent base vectors in the deformed state can therefore be expressed as

for isotropic part:

$$\hat{\mathbf{g}}_1 = \lambda_1 \cos\alpha \hat{\mathbf{m}} + \lambda_1 \sin\alpha \hat{\mathbf{b}}, \quad (\hat{\mathbf{g}}_2)_{iso} = \sqrt{\frac{p_h}{A_1}}\left(-\cos\phi \hat{\mathbf{b}} + \sin\phi \hat{\mathbf{t}}\right), \tag{91}$$

$$(\hat{\mathbf{g}}_3)_{iso} = \sqrt{\frac{p_h}{A_1}}\left(\sin\phi \hat{\mathbf{b}} + \cos\phi \hat{\mathbf{t}}\right), \quad \hat{\mathbf{m}} = \cos(\varphi+\theta)\mathbf{i}_1 + \sin(\varphi+\theta)\mathbf{i}_2,$$

for anisotropic part:

$$\hat{\mathbf{g}}_1 = \lambda_1 \cos\alpha \hat{\mathbf{m}} + \lambda_1 \sin\alpha \hat{\mathbf{b}}, \quad (\hat{\mathbf{g}}_2)_{aniso} = (\lambda_2)_{aniso}\left(-\cos\phi \hat{\mathbf{b}} + \sin\phi \hat{\mathbf{t}}\right),$$
$$(\hat{\mathbf{g}}_3)_{aniso} = (\lambda_3)_{aniso}\left(\sin\phi \hat{\mathbf{b}} + \cos\phi \hat{\mathbf{t}}\right), \qquad \hat{\mathbf{m}} = \cos(\varphi+\theta)\mathbf{i}_1 + \sin(\varphi+\theta)\mathbf{i}_2. \tag{92}$$

Using Eq. (91) for isotropic part or Eq. (92) for anisotropic part, the deformation gradient tensor for the uniaxial/plane stress Timoshenko beam problem can therefore be given by

for isotropic part:

$$\mathbf{F}_{iso} = \begin{bmatrix} \lambda_1 \cos(\varphi+\theta)\cos\alpha & -\sin\theta\sin\phi\sqrt{\frac{p_h}{A_1}} & -\sin\theta\cos\phi\sqrt{\frac{p_h}{A_1}} \\ \lambda_1 \sin(\varphi+\theta)\cos\alpha & \cos\theta\sin\phi\sqrt{\frac{p_h}{A_1}} & \cos\theta\cos\phi\sqrt{\frac{p_h}{A_1}} \\ \lambda_1 \sin\alpha & -\cos\phi\sqrt{\frac{p_h}{A_1}} & \sin\phi\sqrt{\frac{p_h}{A_1}} \end{bmatrix} \tag{93}$$

with volume invariant

$$J_{iso} = \lambda_1 \cos\varphi\cos\alpha \frac{p_h}{A_1} \tag{94}$$

for anisotropic part:

$$\mathbf{F}_{aniso} = \begin{bmatrix} \lambda_1 \cos(\varphi+\theta)\cos\alpha & -(\lambda_2)_{aniso}\sin\theta\sin\phi & -(\lambda_3)_{aniso}\sin\theta\cos\phi \\ \lambda_1 \sin(\varphi+\theta)\cos\alpha & (\lambda_2)_{aniso}\cos\theta\sin\phi & (\lambda_3)_{aniso}\cos\theta\cos\phi \\ \lambda_1 \sin\alpha & -(\lambda_2)_{aniso}\cos\phi & (\lambda_3)_{aniso}\sin\phi \end{bmatrix} \tag{95}$$

with volume invariant

$$J_{aniso} = \lambda_1 (\lambda_2)_{aniso}(\lambda_3)_{aniso}\cos\varphi\cos\alpha = \frac{K_{51}\cos\varphi\cos\alpha}{G_1\lambda_1\sqrt{\left(1-\cos^2\varphi_{12}\right)\left(1-\cos^2\varphi_{13}\right)}}. \tag{96}$$

The deformation of the cross-section can also be defined by using displacements where the cross-section displaces as a plane of Timoshenko beam but is stretched within its own plane (see Fig. 6 and Fig. 7). At the centroidal axis (y&z = 0), the displacements are defined by

$$u_1\left(x,0,0\right)=u_0(x),\quad u_2\left(x,0,0\right)=v(x),\quad u_3\left(x,0,0\right)=0 \tag{97}$$

where $u_0(x)$ and $v(x)$ are the longitudinal (in direction 1 or x) and transverse (in direction 2 or y) displacements of the centroidal axis, respectively. The displacement functions in the x, y and z directions are herein assumed to be

$$\begin{aligned} u_1 &= u_0(x)-p_y\left(x,y,z\right)\sin\theta \\ u_2 &= v(x)+p_y\left(x,y,z\right)\cos\theta - y \\ u_3 &= p_z\left(x,y,z\right)-z \end{aligned} \tag{98}$$

with the required conditions at the centroid

$$p_y\left(x,0,0\right)=0,\quad p_z\left(x,0,0\right)=0 \tag{99}$$

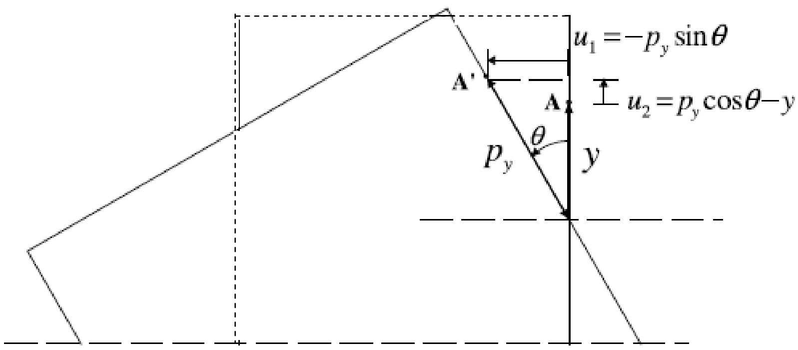

Fig. 7 Deformation of the cross-section in side view [3]

Substituting Eq. (98) into Eq. (8), the deformation gradient tensor defined by using displacements is given by

$$\mathbf{F}=\begin{bmatrix} \left(1+u_{0,x}\right)-p_y\theta,_x\cos\theta-p_{y,x}\sin\theta & -p_{y,y}\sin\theta & -p_{y,z}\sin\theta \\ v,_x-p_y\theta,_x\sin\theta+p_{y,x}\cos\theta & p_{y,y}\cos\theta & p_{y,z}\cos\theta \\ p_{z,x} & p_{z,y} & p_{z,z} \end{bmatrix} \tag{100}$$

The relationship between the displacement gradients and the stretches and deformation angles can then be obtained from Eqs. (93) & (100) for isotropic part and from Eqs. (95) & (100) for anisotropic part as

for isotropic part:

$$
\begin{aligned}
&\lambda_1 \cos(\varphi+\theta)\cos\alpha = (1+u_{0,x}) - (p_y)_{iso}\,\theta,_x \cos\theta - (p_{y,x})_{iso}\sin\theta \\
&\lambda_1 \sin(\varphi+\theta)\cos\alpha = v,_x - (p_y)_{iso}\,\theta,_x \sin\theta + (p_{y,x})_{iso}\cos\theta \\
&\lambda_1 \sin\alpha = (p_{z,x})_{iso}, \quad \sin\phi\sqrt{\frac{p_h}{A_1}} = (p_{y,y})_{iso} = (p_{z,z})_{iso}, \\
&\cos\phi\sqrt{\frac{p_h}{A_1}} = (p_{y,z})_{iso} = -(p_{z,y})_{iso}
\end{aligned}
\tag{101}
$$

with the requirements:

$$
(p_{y,y})^2_{iso} + (p_{z,y})^2_{iso} = \frac{p_h}{A_1}, \quad (p_{z,z})^2_{iso} + (p_{y,z})^2_{iso} = \frac{p_h}{A_1}, \quad (p_{y,y}p_{y,z} + p_{z,z}p_{z,y})_{iso} = 0 \tag{102}
$$

for anisotropic part:

$$
\begin{aligned}
&\lambda_1 \cos(\varphi+\theta)\cos\alpha = (1+u_{0,x}) - (p_y)_{aniso}\,\theta,_x \cos\theta - (p_{y,x})_{aniso}\sin\theta \\
&\lambda_1 \sin(\varphi+\theta)\cos\alpha = v,_x - (p_y)_{aniso}\,\theta,_x \sin\theta + (p_{y,x})_{aniso}\cos\theta \\
&\lambda_1 \sin\alpha = (p_{z,x})_{aniso}, \quad (\lambda_2)_{aniso}\sin\phi = (p_{y,y})_{aniso}, \quad (\lambda_3)_{aniso}\sin\phi = (p_{z,z})_{aniso} \\
&-(\lambda_2)_{aniso}\cos\phi = (p_{z,y})_{aniso}, \quad (\lambda_3)_{aniso}\cos\phi = (p_{y,z})_{aniso}
\end{aligned}
\tag{103}
$$

with the requirements:

$$
\begin{aligned}
&(p_{y,y})^2_{aniso} + (p_{z,y})^2_{aniso} = (\lambda_2)^2_{aniso}, \quad (p_{z,z})^2_{aniso} + (p_{y,z})^2_{aniso} = (\lambda_3)^2_{aniso}, \\
&(p_{y,y}p_{y,z} + p_{z,z}p_{z,y})_{aniso} = 0
\end{aligned}
\tag{104}
$$

Using Eqs. (89), (90), (91), (99) and (103) with an assumption that $p_{y,x}(x,0,0) = 0$, the conponents of the normal and tangential stretches on the plane of the cross-section can be obtained as

$$\lambda_n = \hat{\mathbf{n}} \cdot \hat{\mathbf{g}}_1 = \lambda_1 \cos\varphi \cos\alpha = \lambda_{10} \cos\varphi_0 - p_y \theta,_x$$
$$\lambda_{st} = \hat{\mathbf{t}} \cdot \hat{\mathbf{g}}_1 = \lambda_1 \sin\varphi \cos\alpha = \lambda_{10} \sin\varphi_0 + p_{y,x}$$
$$\lambda_{sb} = \hat{\mathbf{b}} \cdot \hat{\mathbf{g}}_1 = \lambda_1 \sin\alpha = p_{z,x} \tag{105}$$

with

$$\lambda_{10} \cos\varphi_0 = \left(1 + u_{0,x}\right)\cos\theta + v,_x \sin\theta$$
$$\lambda_{10} \sin\varphi_0 = -\left(1 + u_{0,x}\right)\sin\theta + v,_x \cos\theta \tag{106}$$

and

$$\lambda_{10} = \sqrt{\left(1 + u_{0,x}\right)^2 + \left(v,_x\right)^2} \tag{107}$$

where λ_{10} is the longitudinal stretch at the centroid. Using Eq. (106), the shear angle at the centroid and the centroidal axis curvature are given by

$$\tan\left(\theta + \varphi_0\right) = \frac{v,_x}{1 + u_{0,x}}$$
$$\frac{d\theta}{dx} + \frac{d\varphi_0}{dx} = \frac{\left[v,_{xx}\left(1 + u_{0,x}\right) - v,_x u_{0,xx}\right]}{\left(1 + u_{0,x}\right)^2} \tag{108}$$

Using Eq. (105), the stretch λ_1 can be written in terms of the normal and shear stretch components as

$$\left(\lambda_1\right)^2 = \left(\lambda_1 \cos\varphi \cos\alpha\right)^2 + \left(\lambda_1 \sin\varphi \cos\alpha\right)^2 + \left(\lambda_1 \sin\alpha\right)^2$$
$$= \left(\lambda_{10} \cos\varphi_0 - p_y \theta,_x\right)^2 + \left(\lambda_{10} \sin\varphi_0 + p_{y,x}\right)^2 + \left(p_{z,x}\right)^2 \tag{109}$$

The shear angle φ, which varies through the cross-section, can also be written as

$$\tan\varphi = \frac{\lambda_{10} \sin\varphi_0 + p_{y,x}}{\lambda_{10} \cos\varphi_0 - p_y \theta,_x} \tag{110}$$

4.4.1 Solutions for p_y & p_z

for isotropic part:

For small deformations such that $J_{iso} \approx 1$, $\lambda_{10} \cos\varphi_0$ is close to unity and $\theta,_x$ is very small, therefore with $p_h = A_1 - C_1 \ln J$ and using Eqs. (94) and (105), the hydrostatic stress can be approximated as

$$\frac{p_h}{A_1} \cong \frac{1}{1+2\nu\left(\lambda_1 \cos\varphi \cos\alpha - 1\right)} \cong 1 - 2\nu\left(\lambda_{10}\cos\varphi_0 - 1\right) + 2\nu\left(p_y\right)_{iso}\theta,_x \tag{111}$$

According to Eq. (101), $\left(p_{z,z} = p_{y,y}\right)_{iso} \& \left(p_{z,y} = -p_{y,z}\right)_{iso}$, and using Eq. (111), the partial differential Eq. (102) can be reduced to one equation as

$$\begin{gathered}\left(p_{y,y}\right)_{iso}^2 + \left(p_{y,z}\right)_{iso}^2 \cong 1 - 2\nu\left(\lambda_{10}\cos\varphi_0 - 1\right) + 2\nu\left(p_y\right)_{iso}\theta,_x \\ p_y\left(x,0,0\right) = 0, \quad p_{y,x}\left(x,0,0\right) = 0\end{gathered} \tag{112}$$

A solution for $p_y \,\&\, p_z$ can be obtained as

$$\begin{gathered}\left(p_y\right)_{iso} = y - y\nu\left(\lambda_{10}\cos\varphi_0 - 1\right) + \left(y^2 - z^2\right)\theta,_x \frac{\nu}{2} \\ \left(p_z\right)_{iso} = z - z\nu\left(\lambda_{10}\cos\varphi_0 - 1\right) + zy\nu\theta,_x\end{gathered} \tag{113}$$

As mentioned in [3], the displacements defined by Eq. (98) with the expressions in Eq. (113) depict horizontal lines in beam cross-section becoming curved while vertical lines remain straight with rotating (see Fig. 8). This implies that there is anticlastic tranverse curvature associated with the beam bending. The anticlastic curvature leads to an average vertical displacement different to the vertical displacement of the centroid, that is to first order

$$\frac{\iint_A u_2 dA}{A} = v\left(x\right) + \frac{\nu}{2}\left(\frac{I_{zz} - I_{yy}}{A}\right)\theta,_x \tag{114}$$

where $I_{zz} = \iint_A y^2 dA \,\&\, I_{yy} = \iint_A z^2 dA$ are moment of inertia and $\frac{\nu}{2}\left(\frac{I_{zz} - I_{yy}}{A}\right)\theta,_x$ is the anticlastic term.

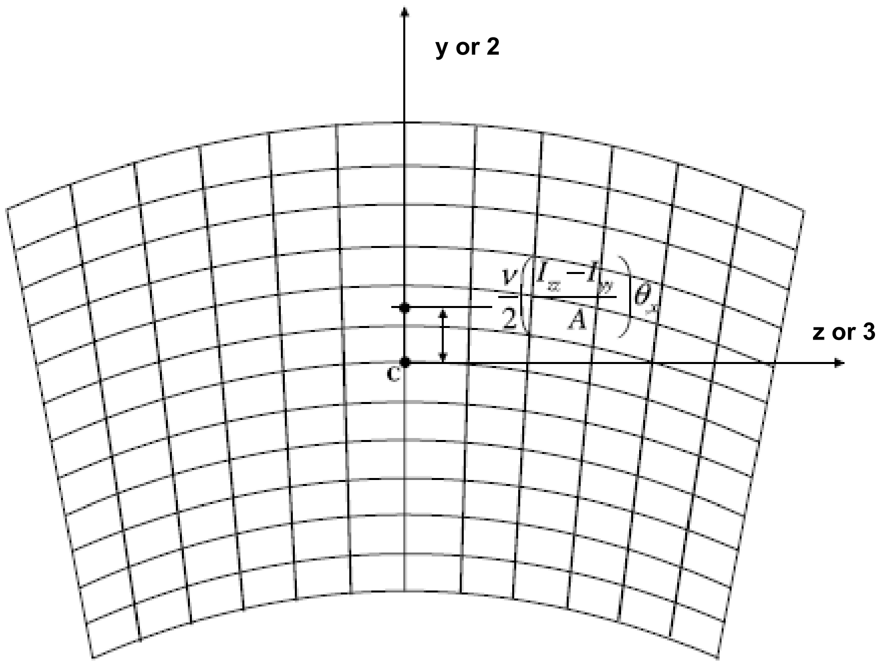

Fig. 8 Anticlastic transverse bending in thick beam cross-section [3]

for anisotropic part:

For small deformations, a Taylor's series expansion of square of Eq. (86)a about $(\lambda_1)^2\left(1-\cos^2\varphi_{12}\right)\approx 1$ and of square of Eq. (86)b about $(\lambda_1)^2\left(1-\cos^2\varphi_{13}\right)\approx 1$ gives for $\left((\lambda_2)^2 \,\&\, (\lambda_3)^2\right)_{aniso}$ the following approximation, respectively

$$\left((\lambda_2)^2\right)_{aniso} \cong \frac{K_{51}}{G_1}\left[2-(\lambda_1)^2\left(1-\cos^2\varphi_{12}\right)\right] \tag{115}$$
$$\left((\lambda_3)^2\right)_{aniso} \cong \frac{K_{51}}{G_1}\left[2-(\lambda_1)^2\left(1-\cos^2\varphi_{13}\right)\right]$$

According to Eq. (103), $\left(p_{z,z}=\frac{\lambda_3}{\lambda_2}p_{y,y} \,\&\, p_{z,y}=-\frac{\lambda_2}{\lambda_3}p_{y,z}\right)_{aniso}$, the partial differential Eq. (104) can be reduced to one equation as

$$\left((\lambda_3)^2\left(p_{y,y}\right)^2+(\lambda_2)^2\left(p_{y,z}\right)^2=(\lambda_2)^2(\lambda_3)^2\right)_{aniso} \tag{116}$$
$$p_y(x,0,0)=0, \quad p_{y,x}(x,0,0)=0$$

Using Eq. (115), Eq. (116) can be approximated as

$$\left[2-(\lambda_1)^2\left(1-\cos^2\varphi_{13}\right)\right]\left(p_{y,y}\right)^2_{aniso}+\left[2-(\lambda_1)^2\left(1-\cos^2\varphi_{12}\right)\right]\left(p_{y,z}\right)^2_{aniso}$$
$$\cong\frac{K_{51}}{G_1}\left[2-(\lambda_1)^2\left(1-\cos^2\varphi_{12}\right)\right]\left[2-(\lambda_1)^2\left(1-\cos^2\varphi_{13}\right)\right]$$
$$p_y\left(x,0,0\right)=0,\quad p_{y,x}\left(x,0,0\right)=0 \tag{117}$$

A solution for p_y & p_z can be approximated as

$$\left(p_y\right)_{aniso}=y\left(\lambda_2\right)_{aniso}=y\sqrt{\frac{K_{51}}{G_1}\left[2-(\lambda_1)^2\left(1-\cos^2\varphi_{12}\right)\right]}$$
$$\left(p_z\right)_{aniso}=z\left(\lambda_3\right)_{aniso}=z\sqrt{\frac{K_{51}}{G_1}\left[2-(\lambda_1)^2\left(1-\cos^2\varphi_{13}\right)\right]} \tag{118}$$

4.4.2 Constitutive Relationships for the Internal Actions

Using the Reissner orientation which assumes that the axial force is normal to the cross-section plane and the shear force parallel to this plane (see Fig. 9), rotating the first Piola Kirchhoff stresses through an angle θ gives stresses which are normal and parallel to the cross-sectional plane [3]. Hence using $\mathbf{\Pi F}^T=\mathbf{S}$ and Eqs. (70) and (93) for isotropic part and using $\mathbf{\Pi F}^T=\mathbf{S}$ and Eqs. (75) and (95) for anisotropic part give

for isotropic part:

$$\left(S_R\right)_{iso}=\begin{bmatrix} A_1\lambda_1\cos\varphi\cos\alpha-\frac{p_h}{\lambda_1\cos\varphi\cos\alpha} & A_1\lambda_1\sin\varphi\cos\alpha & A_1\lambda_1\sin\alpha \\ \sqrt{A_1p_h}\left(\tan\varphi\sin\phi-\frac{\tan\alpha\cos\phi}{\cos\varphi}\right) & 0 & 0 \\ \sqrt{A_1p_h}\left(\tan\varphi\cos\phi-\frac{\tan\alpha\sin\phi}{\cos\varphi}\right) & 0 & 0 \end{bmatrix} \tag{119}$$

for anisotropic part:

$$\left(S_R^{11}\right)_{aniso}=\frac{-2D^1e^{B_1\left(K_{51}-1\right)}\cos\varphi\cos\alpha}{\lambda_1\left(\cos^2\varphi_{12}+\cos^2\varphi_{13}-1\right)}$$
$$\cdot\left\{K_{51}-G_1\left[\left((\lambda_2)^2(\lambda_3)^2\right)_{aniso}+(\lambda_1)^2(\lambda_2)^2_{aniso}\cos^2\varphi_{13}+(\lambda_1)^2(\lambda_3)^2_{aniso}\cos^2\varphi_{12}\right]\right\} \tag{120}$$

$$\left(S_R^{12}\right)_{aniso}=\frac{-2D^1e^{B_1\left(K_{51}-1\right)}}{\lambda_1\left(\cos^2\varphi_{12}+\cos^2\varphi_{13}-1\right)}\cdot\left\{\begin{array}{l}K_{51}\left(\sin\varphi\cos\alpha-\cos\phi\cos\varphi_{13}-\sin\phi\cos\varphi_{12}\right)-\\ G_1\left[\begin{array}{l}\left(\left(\lambda_2\right)^2\left(\lambda_3\right)^2\right)_{aniso}\left(\sin\varphi\cos\alpha-\cos\phi\cos\varphi_{13}-\sin\phi\cos\varphi_{12}\right)\\ +\left(\lambda_1\right)^2\left(\lambda_2\right)^2_{aniso}\left(\cos^2\varphi_{13}\left\{\sin\varphi\cos\alpha-\sin\phi\cos\varphi_{12}\right\}+\cos\phi\cos\varphi_{13}\left\{\cos^2\varphi_{12}-1\right\}\right)\\ +\left(\lambda_1\right)^2\left(\lambda_3\right)^2_{aniso}\left(\cos^2\varphi_{12}\left\{\sin\varphi\cos\alpha-\sin\phi\cos\varphi_{13}\right\}+\sin\phi\cos\varphi_{12}\left\{\cos^2\varphi_{13}-1\right\}\right)\end{array}\right]\end{array}\right\} \tag{121}$$

$$\left(S_R^{13}\right)_{aniso}=\frac{-2D^1e^{B_1\left(K_{51}-1\right)}}{\lambda_1\left(\cos^2\varphi_{12}+\cos^2\varphi_{13}-1\right)}\cdot\left\{\begin{array}{l}K_{51}\left(\sin\alpha-\sin\phi\cos\varphi_{13}+\cos\phi\cos\varphi_{12}\right)-\\ G_1\left[\begin{array}{l}\left(\left(\lambda_2\right)^2\left(\lambda_3\right)^2\right)_{aniso}\left(\sin\alpha-\sin\phi\cos\varphi_{13}+\cos\phi\cos\varphi_{12}\right)\\ +\left(\lambda_1\right)^2\left(\lambda_2\right)^2_{aniso}\left(\cos^2\varphi_{13}\left\{\sin\alpha+\cos\phi\cos\varphi_{12}\right\}+\sin\phi\cos\varphi_{13}\left\{\cos^2\varphi_{12}-1\right\}\right)\\ +\left(\lambda_1\right)^2\left(\lambda_3\right)^2_{aniso}\left(\cos^2\varphi_{12}\left\{\sin\alpha-\sin\phi\cos\varphi_{13}\right\}-\cos\phi\cos\varphi_{12}\left\{\cos^2\varphi_{13}-1\right\}\right)\end{array}\right]\end{array}\right\} \tag{122}$$

$$\left(S_R^{21}\right)_{aniso}=\frac{2D^1e^{B_1\left(K_{51}-1\right)}\cos\varphi\cos\alpha\cos\varphi_{12}}{\left(\lambda_2\right)_{aniso}\left(\cos^2\varphi_{12}+\cos^2\varphi_{13}-1\right)}\cdot\left\{K_{51}-G_1\left[\left(\left(\lambda_2\right)^2\left(\lambda_3\right)^2\right)_{aniso}+\left(\lambda_1\right)^2\left(\lambda_2\right)^2_{aniso}\cos^2\varphi_{13}+\left(\lambda_1\right)^2\left(\lambda_3\right)^2_{aniso}\left(1-\cos^2\varphi_{13}\right)\right]\right\} \tag{123}$$

$$\left(S_R^{22}\right)_{aniso}=\frac{2D^1e^{B_1\left(K_{51}-1\right)}}{\left(\lambda_2\right)_{aniso}\left(\cos^2\varphi_{12}+\cos^2\varphi_{13}-1\right)}\cdot\left\{\begin{array}{l}K_{51}\left\{\cos\varphi_{12}\left(\sin\varphi\cos\alpha-\cos\phi\cos\varphi_{13}\right)+\sin\phi\left(\cos^2\varphi_{13}-1\right)\right\}-\\ G_1\left[\begin{array}{l}\left(\left(\lambda_2\right)^2\left(\lambda_3\right)^2\right)_{aniso}\left\{\cos\varphi_{12}\left(\sin\varphi\cos\alpha-\cos\phi\cos\varphi_{13}-\sin\phi\cos\varphi_{12}\right)\right\}\\ +\left(\lambda_1\right)^2\left(\lambda_2\right)^2_{aniso}\left\{\begin{array}{l}\cos\varphi_{12}\cos^2\varphi_{13}\left(\sin\varphi\cos\alpha-\sin\phi\cos\varphi_{12}\right)\\ +\cos\varphi_{12}\cos\phi\cos\varphi_{13}\left(\cos^2\varphi_{12}-1\right)\end{array}\right\}\\ +\left(\lambda_1\right)^2\left(\lambda_3\right)^2_{aniso}\left\{\begin{array}{l}\cos\varphi_{12}\left(\sin\varphi\cos\alpha-\cos\phi\cos\varphi_{13}\right)-\sin\phi\\ +\cos^2\varphi_{13}\left(2\sin\phi-\sin\phi\cos^2\varphi_{13}+\cos\phi\cos\varphi_{12}\cos\varphi_{13}\right)\\ +\sin\varphi\cos\alpha\cos\varphi_{12}\left(1-\cos^2\varphi_{13}\right)\end{array}\right\}\end{array}\right]\end{array}\right\} \tag{124}$$

$$
\left(S_R^{23}\right)_{aniso} = \frac{-2D^1 e^{B_1\left(K_{51}-1\right)}}{\left(\lambda_2\right)_{aniso}\left(\cos^2\varphi_{12}+\cos^2\varphi_{13}-1\right)}
\cdot\left\{\begin{array}{l}
K_{51}\left\{\cos\varphi_{12}\left(\sin\phi\cos\varphi_{13}-\sin\alpha\right)+\cos\phi\left(\cos^2\varphi_{13}-1\right)\right\}- \\
G_1\left[\begin{array}{l}
\left(\left(\lambda_2\right)^2\left(\lambda_3\right)^2\right)_{aniso}\left\{\cos\varphi_{12}\left(\sin\phi\cos\varphi_{13}-\cos\phi\cos\varphi_{12}-\sin\alpha\right)\right\} \\
+\left(\lambda_1\right)^2\left(\lambda_2\right)^2_{aniso}\left\{\begin{array}{l}\cos\varphi_{12}\cos^2\varphi_{13}\left(-\cos\phi\cos\varphi_{12}-\sin\alpha\right) \\ -\cos\varphi_{12}\sin\phi\cos\varphi_{13}\left(\cos^2\varphi_{12}-1\right)\end{array}\right\} \\
+\left(\lambda_1\right)^2\left(\lambda_3\right)^2_{aniso}\left\{\begin{array}{l}\cos\varphi_{12}\left(\sin\phi\cos\varphi_{13}-\sin\alpha\right)-\cos\phi \\ +\cos^2\varphi_{13}\left(2\cos\phi-\cos\phi\cos^2\varphi_{13}\right) \\ +\cos^2\varphi_{13}\left(-\sin\phi\cos\varphi_{12}\cos\varphi_{13}+\sin\alpha\cos\varphi_{12}\right)\end{array}\right\}
\end{array}\right]
\end{array}\right\} \tag{125}
$$

$$
\left(S_R^{31}\right)_{aniso} = \frac{2D^1 e^{B_1\left(K_{51}-1\right)}\cos\varphi\cos\alpha\cos\varphi_{13}}{\left(\lambda_3\right)_{aniso}\left(\cos^2\varphi_{12}+\cos^2\varphi_{13}-1\right)}
\cdot\left\{K_{51}-G_1\left[\left(\left(\lambda_2\right)^2\left(\lambda_3\right)^2\right)_{aniso}+\left(\lambda_1\right)^2\left(\lambda_3\right)^2_{aniso}\cos^2\varphi_{12}+\left(\lambda_1\right)^2\left(\lambda_2\right)^2_{aniso}\left(1-\cos^2\varphi_{12}\right)\right]\right\} \tag{126}
$$

$$
\left(S_R^{32}\right)_{aniso} = \frac{2D^1 e^{B_1\left(K_{51}-1\right)}}{\left(\lambda_3\right)_{aniso}\left(\cos^2\varphi_{12}+\cos^2\varphi_{13}-1\right)}
\cdot\left\{\begin{array}{l}
K_{51}\left\{\cos\varphi_{13}\left(\sin\varphi\cos\alpha-\sin\phi\cos\varphi_{12}\right)+\cos\phi\left(\cos^2\varphi_{12}-1\right)\right\}- \\
G_1\left[\begin{array}{l}
\left(\left(\lambda_2\right)^2\left(\lambda_3\right)^2\right)_{aniso}\left\{\cos\varphi_{13}\left(\sin\varphi\cos\alpha-\cos\phi\cos\varphi_{13}-\sin\phi\cos\varphi_{12}\right)\right\} \\
+\left(\lambda_1\right)^2\left(\lambda_2\right)^2_{aniso}\left\{\begin{array}{l}\sin\phi\cos\varphi_{12}\cos\varphi_{13}\left(\cos^2\varphi_{12}-1\right) \\ -\sin\varphi\cos\alpha\cos\varphi_{13}\left(\cos^2\varphi_{12}-1\right) \\ +\cos^2\varphi_{12}\left(2\cos\phi-\cos\phi\cos^2\varphi_{12}\right)-\cos\phi\end{array}\right\} \\
+\left(\lambda_1\right)^2\left(\lambda_3\right)^2_{aniso}\left\{\begin{array}{l}\cos^2\varphi_{12}\cos\varphi_{13}\left(\sin\varphi\cos\alpha-\cos\phi\cos\varphi_{13}\right) \\ +\sin\phi\cos\varphi_{12}\cos\varphi_{13}\left(\cos^2\varphi_{13}-1\right)\end{array}\right\}
\end{array}\right]
\end{array}\right\} \tag{127}
$$

$$\left(S_R^{33}\right)_{aniso} = \frac{2D^1 e^{B_1\left(K_{51}-1\right)}}{\left(\lambda_3\right)_{aniso}\left(\cos^2\varphi_{12}+\cos^2\varphi_{13}-1\right)} \tag{128}$$

$$\cdot\left\{\begin{array}{l} K_{51}\left\{\cos\varphi_{13}\left(\cos\phi\cos\varphi_{12}+\sin\alpha\right)+\sin\phi\left(\cos^2\varphi_{12}-1\right)\right\}- \\ G_1\left[\begin{array}{l} \left(\left(\lambda_2\right)^2\left(\lambda_3\right)^2\right)_{aniso}\left\{\cos\varphi_{13}\left(\cos\phi\cos\varphi_{12}+\sin\alpha-\sin\phi\cos\varphi_{13}\right)\right\} \\ +\left(\lambda_1\right)^2\left(\lambda_2\right)^2_{aniso}\left\{\begin{array}{l} -\cos\phi\cos\varphi_{12}\cos\varphi_{13}\left(\cos^2\varphi_{12}-1\right) \\ -\sin\alpha\cos\varphi_{13}\left(\cos^2\varphi_{12}-1\right) \\ +\cos^2\varphi_{12}\left(2\sin\phi-\sin\phi\cos^2\varphi_{12}\right)-\sin\phi \end{array}\right\} \\ +\left(\lambda_1\right)^2\left(\lambda_3\right)^2_{aniso}\left\{\begin{array}{l} \cos^2\varphi_{12}\cos\varphi_{13}\left(\sin\alpha-\sin\phi\cos\varphi_{13}\right) \\ -\cos\phi\cos\varphi_{12}\cos\varphi_{13}\left(\cos^2\varphi_{13}-1\right) \end{array}\right\} \end{array}\right] \end{array}\right\}$$

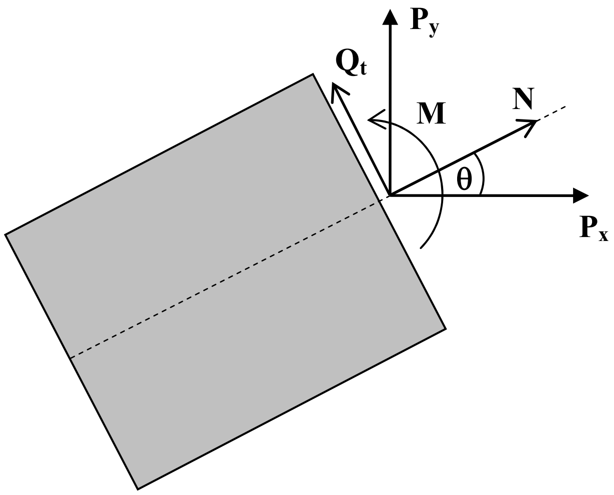

Fig. 9 Beam internal actions

The constitutive relationships for the internal actions can be determined by defining the internal actions as the stress resultants over the cross-section as

for isotropic part:

$$\begin{aligned} \left(N\right)_{iso} &= \iint_A \left(S_R^{11}\right)_{iso} dA, \quad \left(Q_t\right)_{iso} = \iint_A \left(S_R^{12}\right)_{iso} dA, \\ \left(Q_b\right)_{iso} &= \iint_A \left(S_R^{13}\right)_{iso} dA = 0, \quad \left(M\right)_{iso} = \iint_A -p_y \left(S_R^{11}\right)_{iso} dA \end{aligned} \tag{129}$$

where N is the axial force perpendicular to the cross-sectional plane in the direction $\hat{\mathbf{n}}$, Q_t is the shear force within the cross-sectional plane in the direction $\hat{\mathbf{t}}$, Q_b is the shear force within the cross-sectional plane in the direction $\hat{\mathbf{b}}$ and M is the bending moment resulting from the stress perpendicular to the cross-sectional plane (see Fig. 9). Substituting Eq. (119) with Eq. (105), (111) and (113) into (129) and assuming that $\left(\lambda_1\right)_{iso}\cos\varphi\cos\alpha$ is close to unity and $\theta_{,x}$ is very small, gives (to first order)

$$\begin{aligned}&\left(N\right)_{iso}\approx EA\left(\lambda_{10}\cos\varphi_0-1\right),\\&\left(Q_t\right)_{iso}\approx GA\lambda_{10}\cos\varphi_0+\frac{1}{2}\nu G\left(I_{zz}-I_{yy}\right)\theta_{,xx},\quad\left(M\right)_{iso}\approx EI_{zz}\theta_{,x}\end{aligned}\tag{130}$$

For a stability analysis, the constitutive relationships for the internal actions to second order terms are normally used and can be obtained as

$$\begin{aligned}&\left(N\right)_{iso}\approx EA\left(u_{0,x}+\frac{1}{2}v_{,x}^2-\frac{1}{2}\varphi_0^2\right),\\&\left(Q_t\right)_{iso}\approx GA\left(1+u_{0,x}\right)\varphi_0+\frac{1}{2}\nu G\left(I_{zz}-I_{yy}\right)\theta_{,xx},\quad\left(M\right)_{iso}\approx EI_{zz}\theta_{,x}\end{aligned}\tag{131}$$

Using the Ziegler orientation which assumes that the normal force N_{t0} is directed along the centroidal axis while the shear force Q_{t0} is perpendicular to the centroidal axis of the beam, the constitutive relationships are given by

$$\left(N_{t0}\right)_{iso}\approx EA\left(u_{0,x}+\frac{1}{2}v_{,x}^2-\frac{1}{2}\varphi_0^2\right)+GA\left(1+u_{0,x}\right)\varphi_0^2+\frac{1}{2}\nu G\left(I_{zz}-I_{yy}\right)\varphi_0\theta_{,xx},\tag{132}$$

$$\left(Q_{t0}\right)_{iso}\approx GA\left(1+u_{0,x}\right)\varphi_0+\frac{1}{2}\nu G\left(I_{zz}-I_{yy}\right)\theta_{,xx}-EAu_{0,x}\varphi_0\tag{133}$$

From Eqs. (131) to (133), the simple expressions can be obtained as

$$\left(N_{t0}\right)_{iso}\approx\left(N\right)_{iso}+\left(Q_t\right)_{iso}\varphi_0,\quad\left(Q_{t0}\right)_{iso}\approx\left(Q_t\right)_{iso}-\left(N\right)_{iso}\varphi_0\tag{134}$$

for anisotropic part:

$$\begin{aligned}&\left(N\right)_{aniso}=\iint_A\left(S_R^{11}\right)_{aniso}dA,\quad\left(Q_t\right)_{aniso}=\iint_A\left(S_R^{12}\right)_{aniso}dA,\\&\left(Q_b\right)_{aniso}=\iint_A\left(S_R^{13}\right)_{aniso}dA=0,\quad\left(M\right)_{aniso}=\iint_A-p_y\left(S_R^{11}\right)_{aniso}dA\end{aligned}\tag{135}$$

Substituting Eqs. (120) to (122) with Eq. (115) into (155) gives (to first order)

$$\left(N\right)_{aniso} \approx \frac{-2D^1 e^{B_1\left(K_{51}-1\right)} K_{51} A \cos\varphi \cos\alpha}{\lambda_1 G_1 \left(\cos^2\varphi_{12} + \cos^2\varphi_{13} - 1\right)} \cdot \begin{bmatrix} G_1 - 4K_{51}\left(1-\left(\lambda_1\right)^2\right) \\ -2\left(\cos^2\varphi_{12} + \cos^2\varphi_{13}\right)\left(\left(\lambda_1\right)^2 + K_{51}\lambda_1\right) \end{bmatrix} \tag{136}$$

$$\left(Q_t\right)_{aniso} \approx \frac{-2D^1 e^{B_1\left(K_{51}-1\right)} K_{51} A}{\lambda_1 G_1 \left(\cos^2\varphi_{12} + \cos^2\varphi_{13} - 1\right)} \cdot \begin{bmatrix} \left(G_1 - 4K_{51}\right)\left\{\sin\varphi\cos\alpha - \cos\phi\cos\varphi_{13} - \sin\phi\cos\varphi_{12}\right\} \\ +2\left(\lambda_1\right)^2 G_1\left\{\sin\phi\cos\varphi_{12} - \sin\varphi\cos\alpha\left(\cos^2\varphi_{12} + \cos^2\varphi_{13}\right)\right\} \\ +2K_{51}\left(\lambda_1\right)^2\begin{Bmatrix} \sin\varphi\cos\alpha\left(2-\cos^2\varphi_{12} - \cos^2\varphi_{13}\right) - \cos\phi\cos\varphi_{13}\left(2-\cos^2\varphi_{12} - \cos\varphi_{13}\right) \\ -\sin\phi\cos\varphi_{12}\left(2-\cos\varphi_{12} - \cos^2\varphi_{13}\right) \end{Bmatrix} \end{bmatrix}$$

$$\left(M\right)_{aniso} \approx y\sqrt{\frac{K_{51}}{G_1}\left\{2-\left(\lambda_1\right)^2\left(1-\cos^2\varphi_{12}\right)\right\}} \frac{2D^1 e^{B_1\left(K_{51}-1\right)} K_{51} A \cos\varphi \cos\alpha}{\lambda_1 G_1 \left(\cos^2\varphi_{12} + \cos^2\varphi_{13} - 1\right)} \cdot \begin{bmatrix} G_1 - 4K_{51}\left(1-\left(\lambda_1\right)^2\right) \\ -2\left(\cos^2\varphi_{12} + \cos^2\varphi_{13}\right)\left(\left(\lambda_1\right)^2 + K_{51}\lambda_1\right) \end{bmatrix}$$

4.4.3 Equilibrium and Virtual Work

Using the Reissner stresses, the equilibrium Eq. (77) for the beam problem can be expressed as

$$\begin{aligned} \frac{\partial S_R^{11}}{\partial x} + \frac{\partial S_R^{21}}{\partial y} + \frac{\partial S_R^{31}}{\partial z} &= 0 \\ \frac{\partial S_R^{12}}{\partial x} + \frac{\partial S_R^{22}}{\partial y} + \frac{\partial S_R^{32}}{\partial z} &= 0 \\ \frac{\partial S_R^{13}}{\partial x} + \frac{\partial S_R^{23}}{\partial y} + \frac{\partial S_R^{33}}{\partial z} &= 0 \end{aligned} \tag{137}$$

And the equilibrium Eq. (78) becomes

$$
\begin{aligned}
&-S_R^{11}\lambda_1\sin\varphi\cos\alpha+S_R^{12}\lambda_1\cos\varphi\cos\alpha=S_R^{21}\lambda_2\sin\phi+S_R^{31}\lambda_3\cos\phi \\
&S_R^{12}\lambda_1\sin\alpha-S_R^{13}\lambda_1\sin\varphi\cos\alpha=S_R^{22}\lambda_2\cos\phi+S_R^{23}\lambda_2\sin\phi-S_R^{32}\lambda_3\sin\phi+S_R^{33}\lambda_3\cos\phi \\
&S_R^{21}\lambda_2\left(\tan\phi\tan\alpha+\sin\varphi\right)-S_R^{31}\lambda_3\left(\tan\phi\sin\varphi-\tan\alpha\right)=S_R^{22}\lambda_2\cos\varphi \\
&\qquad\qquad+S_R^{23}\lambda_2\tan\phi\cos\varphi-S_R^{32}\lambda_3\tan\phi\cos\varphi+S_R^{33}\lambda_3\cos\varphi
\end{aligned}
\tag{138}
$$

In addition, the virtual work can be expressed in terms of the Reissner stresses as

$$
\begin{aligned}
\delta U=\iiint_V&\begin{bmatrix}S_R^{11}\delta\left(\lambda_1\cos\varphi\cos\alpha\right)+S_R^{12}\delta\left(\lambda_1\sin\varphi\cos\alpha\right)\\ +S_R^{13}\delta\left(\lambda_1\sin\alpha\right)+\left(S_R^{13}\lambda_1\sin\varphi\cos\alpha-S_R^{12}\lambda_1\sin\alpha\right)\delta\phi\end{bmatrix}dV \\
&-\iint_S\mathbf{p}\delta\mathbf{u}dS=0
\end{aligned}
\tag{139}
$$

Noting that, $\lambda_n=\lambda_1\cos\varphi\cos\alpha,\lambda_{st}=\lambda_1\sin\varphi\cos\alpha,\lambda_{sb}=\lambda_1\sin\alpha$ as expressed in Eq. (105). Substituting Eq. (105) into Eq. (139) gives

$$
\iiint_V\begin{bmatrix}S_R^{11}\delta\left(\lambda_{10}\cos\varphi_0\right)-S_R^{11}p_y\delta\theta_{,x}-S_R^{11}\theta_{,x}\delta p_y+S_R^{12}\delta\left(\lambda_{10}\sin\varphi_0\right)\\ +S_R^{12}\delta p_{y,x}+S_R^{13}\delta p_{z,x}+\left\{S_R^{13}\left(\lambda_{10}\sin\varphi_0+p_{y,x}\right)-S_R^{12}p_{z,x}\right\}\delta\phi\end{bmatrix}dV=\iint_S\mathbf{p}\delta\mathbf{u}dS
\tag{140}
$$

Using Eq. (106) and $N=\iint_A S_R^{11}dA,\ Q_t=\iint_A S_R^{12}dA,\ Q_b=\iint_A S_R^{13}dA,\ M=\iint_A -p_yS_R^{11}dA$, an approximation of Eq. (140) is given by

$$
\int_0^L\left[P_x\delta u_{0,x}+P_y\delta v_{,x}-\lambda_{10}Q_{t0}\delta\theta+M\delta\theta_{,x}+\lambda_{10}Q_{b0}\delta\phi\right]dx=\iint_S\mathbf{p}\delta\mathbf{u}dS
\tag{141}
$$

In which

$$
\begin{aligned}
&P_x=N\cos\theta-Q_t\sin\theta,\quad P_y=N\sin\theta+Q_t\cos\theta,\\
&Q_{t0}=-N\sin\varphi_0+Q_t\cos\varphi_0,\quad Q_{b0}=Q_b\sin\varphi_0
\end{aligned}
\tag{142}
$$

P_x and P_y are the internal force resultants in the x and y directions (see Fig. 9), respectively, while Q_{b0} is the shear resultants perpendicular to Q_{t0} with Ziegler orientation. In addition, another simple form of the virtual work can be obtained by using Eq. (140) with $N=\iint_A S_R^{11}dA,\ Q_t=\iint_A S_R^{12}dA,\ Q_b=\iint_A S_R^{13}dA,\ M=\iint_A -p_yS_R^{11}dA$ as

$$
\int_0^L\left[N\delta\left(\lambda_{10}\cos\varphi_0\right)+Q_t\delta\left(\lambda_{10}\sin\varphi_0\right)+M\delta\theta_{,x}+Q_b\lambda_{10}\sin\varphi_0\delta\phi\right]dx=\iint_S\mathbf{p}\delta\mathbf{u}dS
\tag{143}
$$

$$\int_0^L \left[N_{t0}\delta\lambda_{10} + Q_{t0}\lambda_{10}\delta\varphi_0 + M\,\delta\theta_{,x} + Q_{b0}\lambda_{10}\delta\phi \right] dx = \iint_S \mathbf{p}\delta\mathbf{u}dS \tag{144}$$

4.4.4 Column Buckling

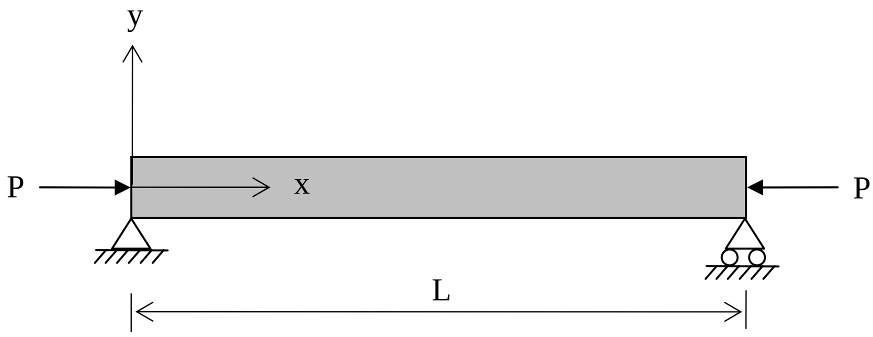

Fig. 10 Simple column under uniaxial load

Consider a straight prismatic simply supported column (see Fig. 10) under initial uniform axial stress $S_R^{11} = -\frac{P}{A}$ where P is the axial force. Using Eq. (144) with Eq. (137), (138) and $N_{t0} \approx N + Q_t\varphi_0$, $Q_{t0} \approx Q_t - N\varphi_0$, $Q_{b0} = Q_b$, the second variation of work for the Timoshenko beam can be obtained as

$$\delta^2 U = \int_0^L \begin{bmatrix} -P\delta^2\lambda_{10} + \dfrac{1}{2}\delta N_{t0}\delta\lambda_{10} + \dfrac{1}{2}\bar{\lambda}_{10}\delta Q_t\delta\varphi_0 \\ +\dfrac{1}{2}P\bar{\lambda}_{10}\delta^2\varphi_0 + \dfrac{1}{2}\delta M\,\delta\theta_{,x} + \dfrac{1}{2}\bar{\lambda}_{10}\delta Q_b\delta\phi \end{bmatrix} dx - \iint_S \mathbf{p}\delta^2\mathbf{u}dS \tag{145}$$

in which

$$\bar{\lambda}_{10} = 1 + \bar{u}_{0,x}, \quad \delta\lambda_{10} = \delta u_{0,x}, \quad \delta^2\lambda_{10} = \frac{1}{2}\frac{\left(\delta v_{,x}\right)^2}{1+\bar{u}_{0,x}}, \quad \delta v_{,x} = \left(1+\bar{u}_{0,x}\right)\left(\delta\varphi_0 + \delta\theta\right) \tag{146}$$

In order to simplify the formulation, the following approximations are adopted.

$$\begin{aligned} &N_{t0} \approx w_0\left(N_{t0}\right)_{iso} + \left(1-w_0\right)\left(N_{t0}\right)_{aniso}, \left(N_{t0}\right)_{aniso} \approx \beta_N\left(N_{t0}\right)_{iso} \\ &Q_t \approx w_0\left(Q_t\right)_{iso} + \left(1-w_0\right)\left(Q_t\right)_{aniso}, \left(Q_t\right)_{aniso} \approx \beta_{Qt}\left(Q_t\right)_{iso} \\ &M \approx w_0\left(M\right)_{iso} + \left(1-w_0\right)\left(M\right)_{aniso}, \left(M\right)_{aniso} \approx \beta_M\left(M\right)_{iso} \\ &Q_b \approx \left(1-w_0\right)\left(Q_b\right)_{aniso}, \left(Q_b\right)_{aniso} \approx \beta_{Qb}\left(Q_t\right)_{iso} \end{aligned} \tag{147}$$

Substituting Eqs. (131), (132), (146) and (147) into Eq. (145), the second variation of work for the Timoshenko beam becomes

$$\delta^2 U = \int_0^L \begin{bmatrix} -\frac{P}{2}\left(1+\bar{u}_{0,x}\right)\left\{\left(\delta\theta+\delta\varphi_0\right)^2-\left(\delta\varphi_0\right)^2\right\}+\frac{1}{2}\left(w_0+\beta_N-\beta_N w_0\right)EA\left(\delta u_{0,x}\right)^2 \\ +\frac{1}{2}\left(w_0+\beta_M-\beta_M w_0\right)EI_{zz}\left(\delta\theta_{,x}\right)^2+\frac{1}{2}\left(w_0+\beta_{Qt}-\beta_{Qt} w_0\right)GA\left(1+\bar{u}_{0,x}\right)^2\left(\delta\varphi_0\right)^2 \\ +\frac{1}{2}\left(\beta_{Qtb}-\beta_{Qb} w_0\right)GA\left(1+\bar{u}_{0,x}\right)^2\delta\varphi_0\delta\phi \\ +\frac{1}{4}\left(w_0+\beta_{Qt}-\beta_{Qt} w_0\right)\nu G\left(I_{zz}-I_{yy}\right)\left(1+\bar{u}_{0,x}\right)\delta\theta_{,xx}\delta\varphi_0 \\ +\frac{1}{4}\left(\beta_{Qtb}-\beta_{Qb} w_0\right)\nu G\left(I_{zz}-I_{yy}\right)\left(1+\bar{u}_{0,x}\right)\delta\theta_{,xx}\delta\phi \end{bmatrix} dx - \iint_S \mathbf{p}\delta^2\mathbf{u}\,dS \tag{148}$$

4.4.5 Column Buckling Formula

In this section, the buckling load formula for a simple column as shown in Fig. 10 is derived. Assuming $\bar{u}_{0,x} \approx \frac{-P}{EA}$, ignoring the axial rigidity terms and the anticlastic terms, the second variation Eq. (148) is simplified as

$$\delta^2 U = \int_0^L \begin{bmatrix} -\frac{P}{2}\left(1-\frac{P}{EA}\right)\left\{\left(\delta\theta+\delta\varphi_0\right)^2-\left(\delta\varphi_0\right)^2\right\}+\frac{1}{2}\left(w_0+\beta_M-\beta_M w_0\right)EI_{zz}\left(\delta\theta_{,x}\right)^2 \\ +\frac{1}{2}\left(w_0+\beta_{Qt}-\beta_{Qt} w_0\right)GA\left(1-\frac{P}{EA}\right)^2\left(\delta\varphi_0\right)^2 \\ +\frac{1}{2}\left(\beta_{Qtb}-\beta_{Qb} w_0\right)GA\left(1-\frac{P}{EA}\right)^2\delta\varphi_0\delta\phi \end{bmatrix} dx - \iint_S \mathbf{p}\delta^2\mathbf{u}\,dS \tag{149}$$

The functional Eq. (149) is set to zero in order to determine its lower bound. The following expressions are obtained as the variation symbol has been dropped.

$$\left(w_0+\beta_M-\beta_M w_0\right)EI_{zz}\theta_{,xx} = -P\left(1-\frac{P}{EA}\right)\left(\theta+\varphi_0\right) \tag{150}$$

$$\left(w_0+\beta_{Qt}-\beta_{Qt}w_0\right)GA\left(1-\frac{P}{EA}\right)^2\varphi_0$$
$$+\left(\beta_{Qtb}-\beta_{Qb}w_0\right)GA\left(1-\frac{P}{EA}\right)^2\phi=P\left(1-\frac{P}{EA}\right)\theta \tag{151}$$

Assuming that $\phi=\beta_\phi\theta$, Eqs. (150) and (151) can be rewritten in a simplified form as

$$r^2\theta_{,xx}+b\theta=0,\quad r^2=\frac{I_{zz}}{A} \tag{152}$$

in which

$$b=\frac{1}{\left(w_0+\beta_M-\beta_M w_0\right)}\left\{\begin{array}{l}\dfrac{P}{EA}\left[1-\dfrac{\beta_\phi\left(\beta_{Qtb}-\beta_{Qb}w_0\right)}{\left(w_0+\beta_{Qt}-\beta_{Qt}w_0\right)}\right]\\+\left(\dfrac{P}{EA}\right)^2\left[\dfrac{E}{\left(w_0+\beta_{Qt}-\beta_{Qt}w_0\right)G}+\dfrac{\beta_\phi\left(\beta_{Qtb}-\beta_{Qb}w_0\right)}{\left(w_0+\beta_{Qt}-\beta_{Qt}w_0\right)}-1\right]\end{array}\right\} \tag{153}$$

Applying the boundary conditions for the problem considered, $\theta_{,x}=0$ at $x=0\,\&\,L$, the solution to the differential Eq. (152) for compression loading is obtained as the classical cosine function for the buckling mode bending angle.

$$\theta(x)=c_1\cos\left(\frac{\sqrt{b}x}{r}\right)+c_2\sin\left(\frac{\sqrt{b}x}{r}\right)$$
$$-c_1\frac{\sqrt{b}L}{r}\sin\left(\frac{\sqrt{b}L}{r}\right)=0,\quad c_2=0 \tag{154}$$

The critical buckling load is obtained by assuming that b is real and non-zero, $\frac{\sqrt{b}L}{r}=n\pi$ where n representing the buckling mode number is an integer, as

$$\frac{P_{cr}}{EA}=\frac{1}{2}\left(\frac{1}{1-\frac{E}{\beta_1 G}}\right)\pm\sqrt{\left(\frac{1}{1-\frac{E}{\beta_1 G}}\right)^2-\frac{4n^2P_{euler}\left(w_0+\beta_M-\beta_M w_0\right)\left(w_0+\beta_{Qt}-\beta_{Qt}w_0\right)G}{EA\left(\beta_1 G-E\right)}} \tag{155}$$
$$\beta_1=w_0+\beta_{Qt}-\beta_{Qt}w_0-\beta_\phi\left(\beta_{Qtb}-\beta_{Qb}w_0\right),\quad P_{euler}=\frac{\pi^2EI_{zz}}{L^2}$$

Chapter 5

Conclusions and Recommendations

5.1 Conclusions

In order to obtain buckling equation for anisotropic columns, a generalized strain energy function for anisotropic hyperelastic materials has been derived and proposed in this study. The proposed strain energy function has been verified by comparison to experimental results. The strain energy function was decomposed into an isotropic and anisotropic component. The formulation was based on the framework of the invariant theory and polyconvexity and coercivity conditions. The anisotropy was represented by an isotropic tensor function through the so-called structural tensors. The specific functions for the anisotropic component were presented. The proposed strain energy function was shown to accurately predict the anisotropic stress response of human arterial tissues under uniaxial and biaxial tests. Finally, a simplified buckling equation which includes shear deformations for anisotropic columns has been determined using the proposed strain energy function.

5.2 Recommendations

Some further studies that can be suggested are the following.

- More applications of the proposed model to other materials for further developments.
- To formulate buckling equation by using a consistent hyperelastic formulation.

References

[1] Wempner, G. (1981). *Mechanics of solids with applications to thin bodies*, Sijthoff and Noordhoff, Alpena an den Rijn, The Netherlands.

[2] Flügge, W. (1972). *Tensor analysis and continuum mechanics*, Berlin : Springer.

[3] Attard, M.M. and Hunt, G.W. (2008). "Column buckling with shear deformations - A hyperelastic formulation." *International Journal of Solids and Structures*, 45(14-15), 4322-4339.

[4] SchrÖder, J., Neff, P. and Ebbing, V. (2008). "Anisotropic polyconvex energies on the basis of crystallographic motivated structural tensors." *Journal of the Mechanics and Physics of Solids*, 56(12), 3486-3506.

[5] Truesdell, C. and Noll, W. (1965). "The nonlinear field theories of mechanics." S. Flügge, ed., Handbuch der Physik Bd.III/3. Springer.

[6] Zhang, J.M. and Rychlewski, J. (1990). "Structural tensors for anisotropic solids." *Archives of Mechanics*, 42(3), 267-277.

[7] Spencer, A.J.M. (1971). "Theory of invariants." Continuum Physics, A.C. Eringen, ed., Academic Press, New York, 239–353.

[8] Boehler, J.P. (1987). "Introduction to the invariant formulation of anisotropic constitutive equations." Applications of Tensor Functions in Solid Mechanics, CISM Course no. 292, J.P. Boehler, ed., Springer-Verlag.

[9] Zheng, Q.-S. and Boehler, J.P. (1994). "The description, classification, and reality of material and physical symmetries." *Acta Mechanica*, 102(1), 73-89.

[10] SchrÖder, J. and Neff, P. (2003). "Invariant formulation of hyperelastic transverse isotropy based on polyconvex free energy functions." *International Journal of Solids and Structures*, 40(2), 401-445.

[11] Ball, J.M. (1977). "Convexity conditions and existence theorems in nonlinear elasticity." *Archive of Rational Mechanics and Analysis*, 63, 337-403.

[12] SchrÖder, J., Neff, P. and Balzani, D. (2005). "A variational approach for materially stable anisotropic hyperelasticity." *International Journal of Solids and Structures*, 42(15), 4352-4371.

[13] Boyd, S. and Vandenberghe, L. (2004). *Convex optimization*, Cambridge University Press, Cambridge.

[14] Gasser, T.C., Ogden, R.W. and Holzapfel, G.A. (2006). "Hyperelastic modelling of arterial layers with distributed collagen fibre orientations." *Journal of the Royal Society Interface*, 3(6), 15-35.

[15] Attard, M.M. (2003). "Finite strain--isotropic hyperelasticity." *International Journal of Solids and Structures*, 40(17), 4353-4378.

[16] Mooney, M. (1940). "A theory of large elastic deformation." *Journal of Applied Physics*, 11, 582–592.

[17] Simo, J.C. and Pister, K.S. (1984). "Remarks on rate constitutive equations for finite deformation problems: computational implications." *Computer Methods in Applied Mechanics and Engineering* 46, 201–215.

[18] Attard, M.M. and Hunt, G.W. (2004). "Hyperelastic constitutive modeling under finite strain." *International Journal of Solids and Structures*, 41(18-19), 5327-5350.

[19] Attard, M.M. (2003). "Finite strain--beam theory." *International Journal of Solids and Structures*, 40(17), 4563-4584.

[20] Itskov, M., Ehret, A. and Mavrilas, D. (2006). "A polyconvex anisotropic strain–energy function for soft collagenous tissues." *Biomechanics and Modeling in Mechanobiology*, 5(1), 17-26.

[21] Fung, Y.-C. (1993). *Biomechanics: Mechanical Properties of Living Tissues*, New York: Springer-Verlag.

[22] Holzapfel, G.A., Gasser, T.C. and Ogden, R.W. (2000). "A New Constitutive Framework for Arterial Wall Mechanics and a Comparative Study of Material Models." *Journal of Elasticity*, 61(1), 1-48.

[23] Ehret, A.E. and Itskov, M. (2007). "A polyconvex hyperelastic model for fiber-reinforced materials in application to soft tissues." *Journal of Materials Science*, 42(21), 8853-8863.

[24] Holzapfel, G.A., Sommer, G., Gasser, C.T. and Regitnig, P. (2005). "Determination of layer-specific mechanical properties of human coronary arteries with nonatherosclerotic intimal thickening and related constitutive modeling." *Am J Physiol Heart Circ Physiol*, 289(5), H2048-2058.

[25] Geest, J.P.V., Sacks, M.S. and Vorp, D.A. (2004). "Age Dependency of the Biaxial Biomechanical Behavior of Human Abdominal Aorta." *Journal of Biomechanical Engineering*, 126(6), 815-822.